

**THE APPLICATION OF MONTE CARLO COMBINED METHODS
FOR MODELING OF POLYMERIZATION KINETICS**

by

Mohammad-Ali Parsa

A thesis submitted to the Department of Chemical Engineering
In conformity with the requirements for
the degree of Master of Applied Science

Queen's University
Kingston, Ontario, Canada
September, 2014

Copyright © Mohammad-Ali Parsa, 2014

Abstract

The advantages and disadvantages of the two major categories of numerical methods, deterministic and stochastic approaches, in polymer reaction engineering are discussed. Combinations of methods are suggested in order to take advantage of both techniques. A hybrid deterministic/stochastic approach and a combined stochastic/stochastic method are developed to represent two polymerization systems of interest.

The distribution of functional groups in polymer chains produced in radical copolymerization by starved-feed semibatch operation is simulated using three different methodologies. A deterministic model is formulated to separately track the homopolymer chains that are produced without the desired functionality, a Monte Carlo (MC) model is written to represent the system, and a hybrid deterministic/MC approach is taken using new capabilities within the software package PREDICI.

Two Monte Carlo algorithms (dynamic and static) are combined in order to model and simulate the branch distribution and topology of polymer chains synthesized in hyper-branched polymerization of polyethylene with Pd-diimine catalysts. A sensitivity analysis is conducted in order to investigate the impact of kinetic and stochastic parameters on the branch distribution as well as average chain length. Simulated results show excellent agreement with experimental observations.

Co-Authorship

The majority of the work presented in this thesis was conducted by me under supervision of Dr. Robin Hutchinson. Chapter 3 is a published paper coauthored by Mr. Iurii Kozhan and Dr. Michael Wulkow, who implemented the “hybrid MC/deterministic” algorithm in PREDICI used to model the distribution of functional groups. The “Deterministic counters model (PREDICI)” in Chapter 3 was developed by Dr. Robin Hutchinson.

Acknowledgements

I would like to express my very great appreciation to my supervisor, Dr. Robin Hutchinson, for his patient guidance, enthusiastic encouragement and useful critiques throughout my MASc study at Queen's University. I will never forget the hope and brightness he brought to me when I was disappointed.

I would also like to thank Dr. Michael Wulkow and Mr. Iurii Kozhan from CiT GmbH for their invaluable contribution to publish my first article from my MASc studies, as well as Dr. Paul Van Steenberge from Laboratory for Chemical Technology at Ghent University for his helpful suggestions regarding the second part of my project.

Advice given by Dr. João Soares has been a great help in the progress of part of my thesis. In addition, Dr. Zhibin Ye provided me with very valuable information in his lab at Laurentian University, as well as kindly hosting me in the city of Sudbury. I would like to thank them for their help during my research.

I would also like to extend my thanks to the staff of the Chemical Engineering department at Dupuis Hall for their help in offering me the resources in running the program.

Finally, I wish to thank my parents for their support and encouragement throughout my study. Special thanks to my beloved wife, Negin, for standing beside me and giving me the hope for a brighter future.

Table of Contents

Abstract.....	ii
Co-Authorship.....	iii
Acknowledgements.....	iv
List of Figures.....	vii
List of Tables.....	ix
Chapter 1 Introduction.....	1
Thesis Objective and Outline.....	4
References.....	5
Chapter 2 Literature Review.....	6
References.....	13
Chapter 3 Modeling of Functional Group Distribution in Copolymerization: A Comparison of Deterministic and Stochastic Approaches.....	15
3.1 Introduction.....	15
3.2 Copolymerization Recipe and Kinetic Model.....	20
3.3 Methodology.....	23
3.4 Results and Discussion.....	32
3.5 Conclusions.....	48
References.....	50
Chapter 4 Modeling of Branch Distribution in Chain Walking Polymerization: Combination of two Monte Carlo Techniques.....	51
4.1 Introduction.....	51
4.2 Methodology.....	57
4.2.1 Escobedo's Algorithm.....	57
4.2.2 Implemented Gillespie's Algorithm.....	62
4.3 Results and Discussion.....	70
4.3.1 Sensitivity Analysis: Average Chain Length.....	71
4.3.2 Sensitivity Analysis: Total Number of Branches.....	73
4.3.3 Sensitivity Analysis: Branch Distribution.....	75
4.3.4 Comparison to Experimental Data.....	79

4.3.5 Effect of Changing Pressure During Polymerization	86
4.4 Conclusion	88
References.....	90
Chapter 5 Conclusions and Future Work.....	93
References.....	95
Appendix	96

List of Figures

- Figure 3-1. Time evolution of error determined by comparing deterministic and Monte Carlo-based dead polymer number (—) and weight (—) chain length distributions for an ensemble size of 2000 chains. The dotted lines are linear trend lines representing an averaged error.32
- Figure 3-2. A comparison of standard output from the deterministic (■ ■ ■) and MC (—) simulations of the copolymerization system described in Tables 1 and 2: (a) [BMA] vs time, (b) [GMA] vs time, (c) total radical concentration vs time, (d) number-average (deterministic: ■ ■ ■ ; MC: —) and weight-average (deterministic: ■ ■ ■ ; MC —) MWs vs time.....34
- Figure 3-3. (a) A comparison of the final ($t=14400$ s) polymer chain-length distribution (GPC scale) from the deterministic (■ ■ ■) and MC (—) simulations of the copolymerization system described in Tables 1 and 2. (b) The effect of MC sample size on polymer GPC chain-length distributions.36
- Figure 3-4. Full polymer chain-length distributions (GPC scale) (—) showing: (a) subdistributions of chains with zero GMA units (—), one GMA unit (····), and two GMA units (·-·-·) simulated by MC; (b) subdistributions of chains with zero GMA units (—) and one GMA unit (····) simulated by deterministic “counters” model.40
- Figure 3-5. (a) Fraction of polymer molecules at each chain length with zero (—), one (····), two (·-·-·), three (—), and four or more GMA units (—) calculated from MC simulation output. (b) Fraction of polymer molecules at each chain length with zero (—), one (····), and two or more GMA units (—) simulated by deterministic “counters” model.42
- Figure 3-6. (a) GMA fraction in each chain and (b) overall number chain-length distribution, showing the chains with zero, one, two, and three or more GMA units, calculated for an ensemble size of 2000 molecules using the hybrid PREDICI model.....46
- Figure 3-7. Fraction of total chains with zero, one, two, and three GMA units plotted against reaction time, calculated from simulation output from the hybrid (solid lines) and deterministic “counters” model (dotted lines, tracked for zero and one GMA units only).....48
- Figure 4-1. A schematic representation of ethylene polymerization with branch formation occurring after “chain walking” of the catalyst center along the chain. The two branched structures indicate the effect of changing polymerization conditions.53
- Figure 4-2. Mechanistic model for ethylene polymerization with Pd-diimine catalyst. Kinetics are (1) dissociation of monomer, (2) chain walking, (3) trapping of monomer (association), and (4) insertion of monomer. $K_{eq}(= \frac{k_D}{k_T})$ is the equilibrium rate coefficient for trapping/dissociation, and k_{ins} and k_w are the rate coefficient for insertion, and chain walking (1 for forward and -1 for backward chain walking), respectively56
- Figure 4-3. Flowchart showing the order of events in MC simulation of Pd-diimine-catalyzed chain walking polymerization, Escobedo’s algorithm.....59

Figure 4-4. Effect of varying values of k_{ins}^{end} , P_{ins}^{end} , P_{ins}^{inner} , P_w , m , and K_{eq} on average chain length for reaction times of 1000s (—), 3000s (—), 5000s (—), and 7000s (—)..... 72

Figure 4-5. Effect of increase in values of P_{ins}^{inner} , P_{ins}^{end} , P_w , and m on average total number of branches per 1000 C of chains for reaction times of 1000s (—), 3000s (—), 5000s (—), and 7000s (—)..... 74

Figure 4-6. Branch density profiles in early stages polymerization. Left figure shows profiles for shorter branches and right figure presents profiles for Hx+ and total number of branches. 75

Figure 4-7. Effect of increase in values of P_{ins}^{end} , P_{ins}^{inner} , P_w , and m on branch distribution per 1000 C of chains. Branch type: Me (▪), Et (▪), Pr (▪), Bu (▪), Am (▪), and Hx+ (▪)..... 78

Figure 4-8. Comparison of branch distributions from experimental data (▪) and simulation results (▪) for each polymer in Table 4-7..... 82

Figure 4-9. Sample snapshots of the conformations of polymer macromolecule in Table 4-5. Each polymer consists of 1500 carbons. Each color represents a branch index (branching level). Plots (1) to (4) are related to polymer 1 to 4 in Table 4-5, respectively. 85

Figure 4-10. Sample snapshots of the chain produced in two scenarios: (a) chain formed initially at 1 atm (a.1) followed by further chain growth at 100 atm (a.2); and (b) chain formed initially at 100 atm (b.1) followed by further chain growth at 1 atm (b.2)..... 87

Figure A-1. Sample schematic chain topology of a chain with length of 80. Numbers in the circle show the label of the parent monomer, and numbers without symbols display the branch length..... 97

Figure A-2. Sample schematic chain topology of a chain with length of 80. Numbers in the circle show the label of the parent monomer, numbers in the box show the last monomer label, and numbers without symbols display the branch length. 99

List of Tables

Table 3-1. Semibatch recipe for copolymerization of butyl methacrylate and glycidyl methacrylate. Density values from Wang et al.	21
Table 3-2. Kinetic mechanisms of butyl methacrylate (BMA) /glycidyl methacrylate (GMA) copolymerization. Values of BMA rate coefficients from Wang et al., with GMA assumed to have equal reactivity.	22
Table 3-3. Kinetic mechanisms of butyl methacrylate (BMA, 1) /glycidyl methacrylate (GMA, 2) copolymerization for expanded deterministic “counters” model. (See text for definition of radical and polymer distributions.)	28
Table 3-4. Initial and final MC volumes and simulation times for execution of MC code as a function of number of radicals.	37
Table 3-5. Distribution of GMA units among polymer chains calculated by various modeling approaches for a perfectly controlled copolymerization system with $DP_n=20$ and $F_{GMA}=0.05$	43
Table 4-1. Short chain branch distribution for the best set of simulation parameters of Escobedo’s algorithm, and experimental branch distribution. Me, methyl; Et, ethyl; Pr, propyl; Bu, butyl; Am, amyl; Hx+, hexyl and longer branches.	62
Table 4-2. Kinetic mechanism of ethylene polymerization with Pd-diimine catalyst. Catalyst center is moved in the species specified with asterisk.	64
Table 4-3. Values of ethylene chain walking polymerization rate coefficients reported from Dr. Zhibin Ye’s lab.	65
Table 4-4. The effect of input variables on average chain length, total number of branches and branch distribution for ethylene Pd-diimine-catalyzed polymerization, as determined by a sensitivity analysis. Symbols means: increase (+), decrease(-), and no change (o). Double symbols show high sensitivity.	79
Table 4-5. Polymerization conditions of ethylene polymer experiments set by Ye et al. with Pd-catalysts.	80
Table 4-6. Set of parameters for simulation of polymerization in Table 4-5.	80
Table 4-7. Polymer short chain branching distribution and total number of branches per 1000 C from experimental data (measured by ^{13}C NMR in $CDCl_3$ at 30 °C) and simulation results.	81
Table 4-8. Comparison of experimental and simulated chain length according to the value of k_{ins}^{end}	83

Chapter 1

Introduction

The development of models to represent the kinetics and mechanisms of polymerization has helped scientists achieve increased understanding of the reaction systems and consequently, to improve process operation and product properties. Advances in computer hardware with greater capacity and speed have enabled simulations with fewer computational restrictions. Thus, the creation of new or improved kinetic models remains of interest to researchers in polymer reaction engineering.

Full molecular weight distributions of the growing polymer, conformation of the branched-polymer, or the sequence of monomers in copolymerization create high-dimensional systems of differential equations that cannot be solved analytically. Using non-analytical solutions often requires model reductions and simplifying assumptions for feasible solutions, leading to the development of numerical methods for application to polymer systems. These numerical methods can be placed in two major categories: I. Deterministic methods to solve the resulting set of equations (e.g., discrete weighted Galerkin and discrete Fourier transforms) that, for a specific given input, always return specific results; II. Stochastic (e.g., Monte Carlo) methods that rely on repeated random sampling to obtain a representation of the system.

A simplified radical polymerization system, consisting of initiation, propagation, and termination, demonstrates the problems of using an analytical solution (Equations (1.1) to (1.3)):¹



To track the concentration profiles of all the species in the system and reaction rate coefficients, the system of differential equation can be written as:

$$\frac{d[I]}{dt} = -k_d[I][M] \quad (1.4)$$

$$\frac{d[M]}{dt} = -k_d[I][M] - k_p[M]\sum_r[P_r] \quad (1.5)$$

$$\frac{d[P_1]}{dt} = k_d[I][M] - k_p[M][P_1] - k_t[M][P_1]\sum_r[P_r] \quad (1.6)$$

$$\frac{d[P_s]}{dt} = -k_p[M]([P_s] - [P_{s-1}]) - k_t[P_s]\sum_r[P_r] \quad s \geq 2 \quad (1.7)$$

$$\frac{d[D_s]}{dt} = +\frac{1}{2}k_t\sum_{r=1}^{s-1}[P_r][P_{s-r}] \quad (1.8)$$

Concentration profiles for the initiator I and monomer M as well as the chain length distributions of P_s and D_s have to be calculated (Equations (1.4) to (1.8)). An analytical solution is, however, available for only a few situations e.g., living

polymerization (no termination), and polymerizations in which the quasi-steady-state assumption (QSSA) is made.² Significant computing time may be required for a numerical algorithm to solve the non-linear differential equations in the realistic dimension. Additionally, one may need the analysis of temperature, volume, type of reactor and feeding, and/or a description of polymeric structure such as grafting, branching and cross-linking; consideration of some of these factors in the model will add a new differential or an algebraic dimension to the system that increases the complexity.³

Although deterministic methods are helpful tools to overcome some of these complexities, they often require simplifying assumptions, and/or the achieved results do not contain the desired information in sufficient detail. Monte Carlo methods (MC) can provide more detailed information of a system, but often with increased computational effort. More recently, the important features of both techniques have been captured in combined methods (MC/MC or MC/deterministic), which not only has made efficient modeling of some systems possible for the first time, but also provides a deep insight into characteristics of the final molecules.

Thesis Objective and Outline

The primary goals of this work are to study the combination of MC and deterministic methods (the so-called hybrid-model), and to apply MC methods to the study of polymerization kinetics of a hyperbranched system.

Chapter Two presents a short comparison between deterministic and MC methods, and illustrates the necessity of MC method to obtain certain types of detailed results not possible deterministically. The advantages and disadvantages of MC methods are outlined, and its potential and applications in polymer reaction engineering are reviewed. The chapter finishes by reviewing Gillespie's algorithm, which is the heart of this thesis, and introducing Escobedo's algorithm used for the hyperbranched system described in Chapter Four.

Chapter Three, which is already published, demonstrates the capabilities of a hybrid-model implemented in the new version of the software package PREDICI, and compares the MC and deterministic methods by modeling of the functional group distribution in radical copolymerization of butyl methacrylate (BMA) and glycidyl methacrylate (GMA) in starved-feed semibatch operation.⁴ It is shown that the hybrid-model successfully takes the advantages of a MC method while decreasing simulation time by considering a deterministic representation in parallel.

Chapter Four illustrates the advantages of combining two different MC algorithms, Escobedo's and Gillespie's algorithm, in order to study the branch distribution and kinetics of ethylene polymerization with a Pd-diimine catalyst. The effect of input variables on the branch distributions, average chain length, and total number of branches are studied in a parameter sensitivity analysis.

References

- (1) Initiation equation 1.1 is adjusted to simplify the discussion in the chapter. Initiation of free radical polymerization in Chapter 3 is considered according to standard treatment.
- (2) Zapata-González, I.; Saldívar-Guerra, E.; Flores-Tlacuahuac, A.; Vivaldo-Lima, E.; Ortiz-Cisneros, J. *Can. J. Chem. Eng.* **2012**, *90*, 804–823.
- (3) Wulkow, M. *Macromol. Theory Simulations* **1996**, *5*, 393–416.
- (4) Parsa, M. A.; Kozhan, I.; Wulkow, M.; Hutchinson, R. A. *Macromol. Theory Simulations* **2014**, *23*, 207–217.

Chapter 2

Literature Review

Deterministic and stochastic methods, as two major streams of numerical methods, are required to solve mathematical problems for which analytical solutions do not exist. The method of moments is one of the deterministic numerical techniques commonly used to represent polymerization systems, reducing the infinite set of equations by employing the chain length distribution averages.¹ While a limitation of this method is that only weighted averages of the molecular weight distribution (MWD) are defined, the representation is usually adequate for most cases. Although still one of the most popular approaches to model polymerization and define polymer product, more details may be demanded in the kinetic investigations of some systems; for example, in studying the combined effect of chain-scission and long-chain branching on polymer architecture.² Therefore, if full MWDs or higher distributed quantities (e.g., long chain branching (LCB) as a second distribution) are required, one must search for an alternative method. In addition, the moment method requires extra assumptions when implemented for some systems for which a closed form of the moment equations cannot be formulated.

Some of the disadvantages of the method of moments have been resolved by application of the discrete Galerkin h-p-method to polymer systems, as implemented in the commercial software package PREDICI. The package has gained

widespread use in industry and academia due to its modular approach and flexibility in allowing users to construct complete kinetic models from available reaction step patterns and its ability to represent complete MWDs. The full description of advantages of this method is out of scope of this study and can be read at ref ³. It suffices to mention that although the package reduces the computational effort dramatically and can describe a second distributed quantity such as branching or composition as an average quantity with respect to chain length,^{4,5} a full description of bivariate distributions, even if available with an extended Galerkin h-p method, has only been used in special projects.⁶

The Monte Carlo method (MC) is a stochastic numerical approach to model polymerization that can provide detailed information of all the species in the system, allowing the calculation of full MWD and higher order distributions. “Monte Carlo” typically refers to a class of methods in which simulations are run many times over in order to obtain the distribution of an unknown probabilistic entity.⁷ The technique was first introduced in 1946, a year after the first electronic computer, by S. Ulam and then further developed by Nicolas Metropolis.⁸ The term “Monte Carlo” is general, encompassing various algorithms developed for more specific applications. In 1976, Daniel T. Gillespie proposed a MC algorithm for coupled chemical reactions with stochastic time evolution, now recognized as Gillespie’s algorithm.⁹ The main concept is to assume a sample size so small such that the

number of molecules in the system is a finite value. Therefore in Gillespie's algorithm, the numbers of molecules are used instead of molar concentrations.

All of the interactions between the molecules in the system are defined based on the reaction probability density function. Each time a reaction happens, the number of affected molecules must be updated and stored for post-processing, if necessary. Considering the simple radical polymerization system consisting of initiation, propagation and termination (Equations (1.1) to (1.3)) as an example; if initiation happens (Equation (1.1)), the "number" of initiators and monomers in the system will be reduced each by one, the "number" of polymer radicals will be increased by one, and the respective chain length will be set to one. Similarly, if propagation (Equation (1.2)) occurs to one of the randomly selected polymer radicals in the system, the "number" of monomers will decrease by one unit as well as the chain length of that radical will increase by one. The next event chosen and the time interval between updates are selected by generating uniformly distributed random numbers. Implementation of this technique will be fully discussed in later chapters.

In contrast to deterministic numerical methods, the Gillespie MC technique considers the evolution time of a system as a discrete and stochastic process rather than a continuous parameter. Unlike advanced numerical methods such as the Galerkin h-p algorithm, MC methods are simple in concept and easy to implement,

requiring only basic mathematic knowledge even for problems with high complexity.¹⁰

Furthermore, MC methods are easily parallelizable. Parallelization refers to computer processes in which a simulation/calculation is performed on multiple CPUs/computers at the same time.¹¹ In some algorithms such as Gillespie's, parallelization can also be done by running a set of simulations with identical starting conditions for smaller population and taking the average of quantities, in order to reduce the simulation time of a single simulation with large population.¹² In addition, it is possible to employ the MC method to model a system in which some or all kinetics parameters are unknown, but the fixed probabilities of each happening in the system can be estimated.¹³

MC methods, however, have some disadvantages. Sample sizes (number of reactant molecules) in the order of millions or even billions are required to obtain results within an acceptable precision. Despite the improvements in both computer software (programming) and hardware over the past decade, the intensive calculations happening to the large number of molecules reduces the speed of simulation drastically compared to deterministic methods. This deficiency has eliminated the MC method as a suitable technique for real-time simulation and online control, as they require quick response to the changes in the inputs/system.

In addition, MC methods are step-wise procedures, with the probability of the next event dependent on the previous event in the system. They act similar to a black box; i.e., if one wants to change the input(s), a complete new simulation run from beginning to end will be inevitable.¹¹

MC methods are widely used in engineering, from microelectronics to autonomous robotics. In the field of polymer reaction engineering, MC methods have been applied to various polymerizations including free radical¹⁴ and controlled/living¹⁵⁻¹⁸ systems, in order to provide a deeper insight into the polymeric microstructure of each macromolecule. The in-depth information provided by MC method has helped scientists and researchers to investigate different aspects of polymerization. For example, Chen et al. developed a kinetic MC method to study the relation between topology of isolated molecules produced by chain walking polymerization to their molecular size and conformation,¹³ while Hamzehlou et al. applied MC method in order to investigate the microstructure of acrylic functional copolymers, considering all complexities of acrylate kinetics.¹⁹

The MC method not only can be used as an individual tool to model and simulate polymerization, but has recently been implemented in combination with a deterministic method. Schütte and Wulkow introduced a novel “hybrid” algorithm, utilized in the new version of the software package PREDICI, which uses MC alongside a deterministic approach.²⁰ The hybrid algorithm solves the full

deterministic system using the Galerkin h-p approximation method for chain length distributions (CLDs), and in parallel applies the MC technique to simulate single realizations of the stochastic process underlying chain growth, taking advantage of both modeling approaches. As another example of deterministic/MC method combination, a hybrid simulation approach was developed by Neuhaus et al. to combine the advantages of deterministic and stochastic modeling of complex polymerization networks of LDPE in tubular and autoclave reactors.²¹ The fast deterministic simulation solves the heat and pressure balances and the stochastic simulation provides detailed information about the polymeric microstructure.

Another MC algorithm utilized in this research, termed the Escobedo's algorithm, was developed by Chen et al.¹³ Also a MC method-based algorithm, it uses fixed probabilities, unlike Gillespie's algorithm which tracks changing probabilities over the course of a dynamic simulation. This MC algorithm was developed to simulate the topology and conformational behavior of hyperbranched chains formed by polymerization of ethylene using a Pd-diimine catalyst. While the technique was developed specifically for the Pd-diimine-catalyzed ethylene polymerization, it can be considered as a class of MC methods to model other hyperbranched systems, such as polymerization using α -diimine catalysts,^{22,23} or to study the phase behavior of hyperbranched polymers.²⁴

In this thesis, combinations of Gillespie's MC algorithm with a deterministic method, and with Escobedo's MC algorithm will be presented. It will be shown that the

combined methods provide enhanced capabilities to efficiently describe polymer systems.

References

- (1) Ray, W. H. *J. Macromol. Sci. Part C Polym. Rev.* **1972**, *8*, 1–56.
- (2) Cunningham, M. F.; Hutchinson, R. A. In *Hand book of Radical Polymerization*; Matyjaszewski, K.; Davis, T. P., Eds.; John Wiley and Sons, Inc.: Hoboken, 2002; p. 348.
- (3) Wulkow, M. *Macromol. React. Eng.* **2008**, *2*, 461–494.
- (4) Hutchinson, R. A. *Macromol. Theory Simulations* **2001**, *10*, 144–157.
- (5) Iedema, P. D.; Wulkow, M.; Hoefsloot, H. C. J. *Macromolecules* **2000**, *33*, 7173–7184.
- (6) Deuflhard, P.; Huisinga, W.; Jahnke, T.; Wulkow, M. *SIAM J. Sci. Comput.* **2008**, *30*, 2990–3011.
- (7) Mikhailov, G. A. Monte. *Encyclopedia of Mathematics*, 2001.
- (8) Metropolis, N. *Los Alamos Sci. Spec.* **1987**, 125–130.
- (9) Gillespie, D. T. *J. Comput. Phys.* **1976**, *22*, 403–434.
- (10) Lu, J.; Zhang, H.; Yang, Y. *Die Makromol. Chemie, Theory Simulations* **1993**, *2*, 747–760.
- (11) Schmidt, V. *Metrika* **2006**, *64*, 251–252.
- (12) Chen, Z.; Chen, X.; Shao, Z.; Yao, Z.; Biegler, L. T. *Comput. Chem. Eng.* **2013**, *48*, 175–186.
- (13) Chen, Z.; Gospodinov, I.; Escobedo, F. A. *Macromol. Theory Simulations* **2002**, *11*, 136–146.
- (14) Hamzehlou, S.; Ballard, N.; Carretero, P.; Paulis, M.; Asua, J. M.; Reyes, Y.; Leiza, J. R. *Polymer (Guildf)*. **2014**, *55*, 4801–4811.
- (15) Al-Harathi, M.; Soares, J. B. P.; Simon, L. C. *Macromol. Mater. Eng.* **2006**, *291*, 993–1003.

- (16) Al-Harathi, M.; Soares, J. B. P.; Simon, L. C. *Macromol. React. Eng.* **2007**, *1*, 95–105.
- (17) Tobita, H.; Yanase, F. *Macromol. Theory Simulations* **2007**, *16*, 476–488.
- (18) Payne, K. A.; D’hooge, D. R.; Van Steenberge, P. H. M.; Reyniers, M.-F.; Cunningham, M. F.; Hutchinson, R. A.; Marin, G. B. *Macromolecules* **2013**, *46*, 3828–3840.
- (19) Hamzehlou, S.; Reyes, Y.; Leiza, J. R. *Macromol. React. Eng.* **2012**, *6*, 319–329.
- (20) Schütte, C.; Wulkow, M. *Macromol. React. Eng.* **2010**, *4*, 562–577.
- (21) Neuhaus, E.; Herrmann, T.; Vittorias, I.; Lilge, D.; Mannebach, G.; Gonioukh, A.; Busch, M. *Macromol. Theory Simulations* **2014**.
- (22) Santos, J. P. L.; Castier, M.; Melo, P. A. *Polymer (Guildf)*. **2007**, *48*, 5152–5160.
- (23) Guo, L.; Gao, H.; Li, L.; Wu, Q. *Macromol. Chem. Phys.* **2011**, *212*, 2029–2035.
- (24) Seiler, M. *Fluid Phase Equilib.* **2006**, *241*, 155–174.

Chapter 3

Modeling of Functional Group Distribution in Copolymerization: A

Comparison of Deterministic and Stochastic Approaches

With collaboration of Dr. Michael Wulkow from CiT GmbH, Harry-Wilters Ring 27, 26180 Rastede, Germany; and Mr. Iurii Kozhan from FU Berlin, Institute of Mathematics, Arnimallee 6, 14195 Berlin, Germany.

3.1 Introduction

Over a third of synthetic polymers are produced via free radical polymerization (FRP), with products ranging from high volume materials such as low-density polyethylene and polystyrene to medium and high value products such as solvent-borne or waterborne automotive coatings and water-soluble polymers for pharmaceuticals and cosmetics. A mixture of monomers can be selected to achieve desired end-use properties via the production of copolymer chains with a heterogeneous distribution of repeat units along the backbone. However, while FRP offers great versatility in producing copolymers, the sequencing of monomer units along each chain is stochastically controlled by the random addition of monomers to the growing chain. In some applications, monomer sequencing can have a substantial influence on end-use properties, especially when the copolymers are used as dispersants or surfactants to prepare products such as paper and automotive coatings, personal care products, detergents, inks, pharmaceuticals, etc.¹

While there is significant research in applying controlled/living free radical polymerization to synthesize block and comb copolymers for these applications, many commercial dispersants are still synthesized by FRP using a functional comonomer such as glycidyl methacrylate, (meth)acrylic acid or 2-hydroxyethyl (meth)acrylate. An example presented by Barrett² is the copolymerization of a small amount of glycidyl methacrylate (GMA) with an alkyl methacrylate, followed by esterification of the polymeric epoxide with methacrylic acid to produce pendant unsaturated groups. The resultant macromer is a reactive polymeric stabilizer that can produce graft copolymer *in situ* by copolymerization with other acrylic monomers as part of a non-aqueous dispersion. A similar approach is described in a patent, with the precursor polymer chains produced via starved-feed semibatch polymerization and the functional monomer added so that, on average, each chain produced contains one functional unit.³ This production strategy serves as a basis for the copolymerization example of the current simulation study.

The issue specifically addressed here is the distribution of the functional comonomer units among the polymer chains. As concisely stated in the 1973 paper by Barrett:² “However, the overall efficiency of these types of graft copolymers is still defective due to the random nature of the polymerisation process used in their preparation. This inevitably leads to the simultaneous formation of polymers which either have too many reactive groups or none at all and at best only about half of the material produced functions as a dispersant.” Stockmayer⁴ derived an equation to

describe the instantaneous distribution of chain compositions and chain lengths in radical copolymerization under the long-chain hypothesis, an approach generalized by Tobita⁵ to N monomers. However, these derivations are valid only for cases in which the long chain hypothesis (LCH) and the quasi-steady state approximation (QSSA) hold, and are difficult to apply over the course of a dynamic batch or semibatch polymerization with changing conditions.

With the increased speed of computing, a number of research groups have turned to Monte Carlo (MC) methods to simulate polymer architecture, including comonomer sequencing. For example, Al-Harhi et al. simulate the molecular weight and copolymer composition distributions formed by batch and semibatch atom transfer radical polymerization (ATRP).⁶ Van Steenberge et al. also apply MC modeling to represent gradient copolymers produced by ATRP and derive an index to represent gradient quality from the reaction history of all macromolecular species.⁷ In a work related to the current publication, Hamzehlou et al. use MC techniques to compare batch and semibatch FRP of *n*-butyl acrylate (BA) with 1 mol% of the functional monomer 2-hydroxyethyl methacrylate (HEMA), simulating the effect of operating conditions on the distribution of the HEMA units among the high MW polymer chains; in addition, the distribution of branchpoints arising from BA side reactions is also tracked.⁸

Earlier application of MC techniques to the modeling of polymerization kinetics focused on representation of the complete polymer molecular weight distribution (MWD). However, efficient numerical techniques have been developed to solve the set of deterministic equations describing polymerization kinetics including the full MWD, as described by Wulkow⁹ and Saldívar-Guerra et al.¹⁰ In particular the software package PREDICI[®], employing the discrete Galerkin h-p algorithm, has gained widespread use due to its modular approach and flexibility in allowing users to construct complete kinetic models from available reaction step patterns.⁹ While the package can describe a second distributed quantity such as branching or composition as an average quantity with respect to chain length,^{11,12} a full description of bivariate distributions, even if available with an extended Galerkin h-p-method, has only been used in special projects.¹³ Typical reasons for this are that the computation time increases by each added dimension, and that even a bivariate treatment is not enough for real-life problems. Moreover, all of the required balances related to polymerization kinetics (masses, reactor operation, etc.) cannot be handled easily in higher dimensions. Thus, Schütte and Wulkow have recently developed a method to combine the Galerkin h-p method with MC stochastic techniques.¹⁴ As described in more detail below, this new “hybrid” version of PREDICI has been utilized to calculate the distribution of functional groups among low MW polymer chains.

It should be noted that others have developed numerical techniques to describe bivariate MW and chemical composition distributions in dynamic systems using deterministic methods. Some of the earlier efforts are described by Krallis et al.,¹⁵ who compare performance of a MC algorithm to a numerical solution of the discretized bivariate population balance equations using a two-dimensional fixed pivot technique; it was concluded that an efficient MC technique was easier to implement and also required less computational effort. Recently, Brandolin and Asteasuain¹⁶ present a method to transform population balances using 2D probability generating functions, followed by an a posteriori recovery of the distribution from the transform domain by numerical inversion. However, the technique is also rather complex.

In this work, the distribution of functional groups in polymer chains produced by radical copolymerization by starved-feed semibatch operation is simulated using three different methodologies. Monte Carlo code has been developed for a stochastic simulation of the process, a deterministic model is formulated in PREDICI to separately track the homopolymer chains that are produced without the desired functionality, and the new hybrid deterministic/MC approach in PREDICI is utilized. While the particular copolymerization test case is straightforward, it allows for a good comparison of the advantages and disadvantages of the three simulation approaches.

3.2 Copolymerization Recipe and Kinetic Model

The test case is a simplified version of a recipe from Barsotti et al.,³ scaled to be produced in a 1 L vessel. A mixture of *n*-butyl methacrylate (BMA), functional comonomer glycidyl methacrylate (GMA), and *tert*-butyl peracetate (TBPA) initiator is fed at a constant rate over a 4 h period into a reactor controlled at 138 °C containing xylene solvent. The initial mass of xylene is 200 g and the total mass of monomer/initiator fed to the reactor is 500 g such that the final polymer content in the reactor (assuming full conversion) is 71%. The comonomer mixture contains 5 mol% GMA, with the amount of initiator adjusted to result in a final number-average degree of polymerization (DP_n) of 20 such that there is, on average, one GMA unit per chain. The details of the test case recipe (component amounts and densities) are summarized in Table 3-1. As the polymer formed is denser than the reacting monomers, all models described below consider the volume contraction of polymerization as well as the increasing reactor volume from the semibatch feed.

The set of copolymerization mechanisms in the model, along with corresponding rate coefficients at 138 °C, is summarized in Table 3-2. The BMA rate coefficients provide a good description of BMA homopolymerization¹⁷ and co- and terpolymerization¹⁸ experiments conducted under similar starved-feed semibatch operation. To simplify this study it is assumed that GMA has identical propagation,

termination and transfer kinetics to BMA and that no depropagation occurs; while depropagation has some effect on methacrylate free monomer levels at 138 °C,¹⁷ it will have negligible effect on copolymer composition for this methacrylate/methacrylate polymerization. The terminal model of copolymerization kinetics is assumed, with reactivity ratios set to unity. Thus at all times during the reaction, the monomer and polymer compositions are identical at 5 mol% GMA, as set by the feed composition.

Table 3-1. Semibatch recipe for copolymerization of butyl methacrylate and glycidyl methacrylate. Density values from Wang et al.¹⁷

Component	Initial Mass (g)	Mass Fed over 4 h (g)	MW (g·mol⁻¹)	Density at 138 °C (g·mL⁻¹)
Xylene	200	–	106	0.713
Butyl methacrylate	–	454.1	142	0.786
Glycidyl methacrylate	–	23.9	142	0.786 ^a
TBPA initiator	–	22.0	132	0.885
Polymer	–	–		1.078

^a GMA density assumed equal to BMA.

Table 3-2. Kinetic mechanisms of butyl methacrylate (BMA) /glycidyl methacrylate (GMA) copolymerization. Values of BMA rate coefficients from Wang et al.,¹⁷ with GMA assumed to have equal reactivity.

		Value at 138 °C
Initiation	$I \xrightarrow{k_d} 2fI^\bullet$ $I^\bullet + M_i \xrightarrow{k_{p,ii}} P_1^{i\bullet}$	$k_d (\text{s}^{-1}) = 1.32 \times 10^{-3}$; $f = 0.515$
Propagation	$P_n^{i\bullet} + M_j \xrightarrow{k_{p,ij}} P_{n+1}^{j\bullet}$	$k_{p,ij} (\text{L} \cdot \text{mol}^{-1} \cdot \text{s}^{-1}) = 4.67 \times 10^3$; $i, j = 1, 2$
Chain transfer to monomer	$P_n^{i\bullet} + M_j \xrightarrow{k_{tr,ij}^{\text{mon}}} P_1^{j\bullet} + D_n$	$k_{tr,ij}^{\text{mon}} (\text{L} \cdot \text{mol}^{-1} \cdot \text{s}^{-1}) = 0.266$; $i, j = 1, 2$
Chain transfer to solvent	$P_n^{i\bullet} + S \xrightarrow{C_{s,i} k_{p,ii}} I^\bullet + D_n$	$C_{s,i} = 3.54 \times 10^{-4}$; $i = 1, 2$
Termination		
by combination:	$P_n^{i\bullet} + P_r^{j\bullet} \xrightarrow{(1-\delta)k_{t,\text{cop}}} D_{n+r}$	$k_{t,\text{cop}} (\text{L} \cdot \text{mol}^{-1} \cdot \text{s}^{-1}) = 4.89 \times 10^7$ $\delta = 0.65$
by disproportionation:	$P_n^{i\bullet} + P_r^{j\bullet} \xrightarrow{\delta k_{t,\text{cop}}} D_n + D_r$	

3.3 Methodology

Deterministic Model (PREDICI) The copolymerization mechanisms and rate coefficients for the model summarized in Table 3-2 have been entered in PREDICI.

Monte Carlo Simulation The classic MC algorithm introduced by Gillespie¹⁹ has been implemented, following the methodology described by others.^{7,8,20} The method demands conversion of macroscopic, or experimental, reaction rate coefficients (k^{exp}) to microscopic reaction rate coefficients (k^{MC}) according to the following, with N_A =Avogadro's number, and V_{MC} the MC reaction control volume, calculated as discussed later.

$$k^{\text{MC}} = k^{\text{exp}} \quad \text{for first order reaction} \quad (3.1)$$

$$k^{\text{MC}} = \frac{k^{\text{exp}}}{V_{\text{MC}}N_A} \quad \text{for bimolecular reactions between different species} \quad (3.2)$$

$$k^{\text{MC}} = \frac{2k^{\text{exp}}}{V_{\text{MC}}N_A} \quad \text{for bimolecular reactions between identical species} \quad (3.3)$$

The MC rate of ν th reaction, R_ν , is given by:

$$R_\nu = k^{\text{MC}}C_\nu \quad (3.4)$$

where C_ν is the number of possible combinations between reactants engaged in the ν^{th} reaction. For example, C_ν for the second (initiation) reaction from Table 3-2 is calculated as:

$$C_2 = \binom{n_{I^\bullet}}{1} \binom{n_{M_1}}{1} = n_{I^\bullet} \times n_{M_1} \quad (3.5)$$

where n_{I^\bullet} and n_{M_1} are the number of primary radical and monomer 1 molecules in the system, respectively. The probability of each reaction, P_ν , is defined as:¹⁹

$$P_\nu = \frac{R_\nu}{\sum_{\nu=1}^{N_{\text{rxn}}} R_\nu} \quad (3.6)$$

where N_{rxn} is the total number of reactions in the polymerization mechanistic set of Table 3-2. Two uniformly distributed random numbers, r_1 and r_2 , are generated to

determine the reaction that occurs at the polymerization time and the time step, respectively. Reaction μ happens if the following inequality is satisfied:

$$\sum_{\nu=1}^{\mu-1} P_{\nu} < r_1 \leq \sum_{\nu=1}^{\mu} P_{\nu} \quad (3.7)$$

with the time step, τ , calculated as:

$$\tau = \frac{1}{\sum_{\nu=1}^{N_{\text{rxn}}} R_{\nu}} \ln \left(\frac{1}{r_2} \right) \quad (3.8)$$

An important aspect of the MC technique is the choice of V_{MC} , the control volume size, which should be large enough to produce statistically-valid results. Radicals are the species with the lowest concentration in the system, and it was found that choosing a volume that allowed the fluctuation of the number of radicals to include zero generated error in the results. To avoid this problem, the average radical concentration was chosen as a basis to determine an appropriate control volume size, based upon a concentration ($[P^{\bullet}]_{\text{tot}}$) estimated assuming the quasi-steady state assumption:

$$[P^{\bullet}]_{\text{tot}} = \sum_{i=1}^2 \sum_{n=1} [P_n^{i\bullet}] = \left(\frac{2fk_d[I]}{k_{t,\text{cop}}} \right)^{0.5} \quad (3.9)$$

where $[I]$ is calculated based upon initiator concentration in the feed stream. The initial MC control volume $V_{\text{MC}}(0)$ is then calculated based upon the desired number of radicals in the system (n_{rad}):

$$V_{\text{MC}}(0) = \frac{n_{\text{rad}}}{N_A [P^{\bullet}]_{\text{tot}}} \quad (3.10)$$

For semibatch polymerization, the volume constantly increases as the result of adding the feed stream, and is also affected by the difference between polymer and monomer density. The feed rate of monomer and initiator molecules, \dot{n}_i (molecules of species i per unit time), into the MC control volume is calculated by considering the total amount of material fed ($M_{\text{feed tank}}$) into the actual semibatch system with initial volume $V_{\text{reactor}}(0)$ over feeding time t_{feed} :

$$\dot{n}_i = \frac{w_i^{\text{feed}} \times M_{\text{feed tank}} \times V_{\text{MC}}(0) \times N_A}{Mw_i \times V_{\text{reactor}}(0) \times t_{\text{feed}}} \quad , \quad i = I, M_1, M_2 \quad (3.11)$$

where w_i^{feed} and Mw_i are the mass fraction of species i in the feed stream and molecular weight of species i , respectively. The total volume is updated in each iteration based upon the total number of molecules of each species present in the system and assuming volume additivity, thus automatically correcting for volume contraction due to polymerization. Values for k^{MC} s, dependent on volume, are also updated.

The algorithm was implemented in MATLAB, taking advantages of the package's fast indexing and built-in functions to find and change specific properties in the system, and to handle matrices. Simulation output includes dead polymer and radical matrices which deliver information about the chain-length and the number of $M1$ and $M2$ units in each chain, and profiles matrices that store changes of each variable in the system as a function of reaction time. To minimize computer memory usage and simulation time, all other calculations (such as MW averages) are completed in

the post-processing treatment of the results. The Monte Carlo and all other simulations described in this paper were done using a PC with an Intel® Core™-i7 3.4 GHz processor and 8.00 GB memory.

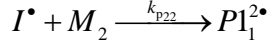
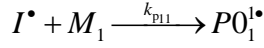
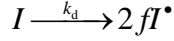
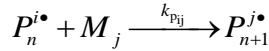
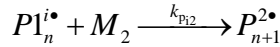
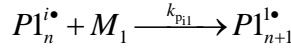
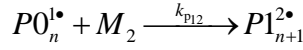
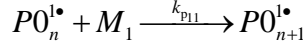
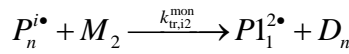
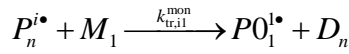
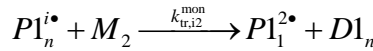
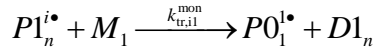
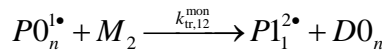
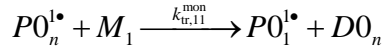
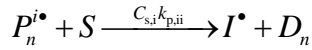
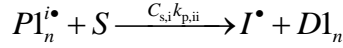
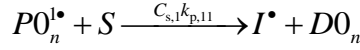
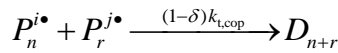
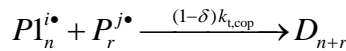
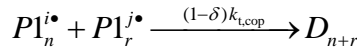
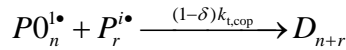
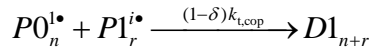
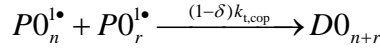
Deterministic “Counters” Model (PREDICI) An alternative way to track the placement of functionality among the polymer chains is to increase the set of distributed species that are tracked in the deterministic model, as summarized in Table 3-3. For this representation we define distributed species D_0 as polymer chains that contain no GMA units (i.e., BMA homopolymer chains), D_1 as those that contain a single GMA unit, and D as chains that contain multiple (two or more) GMA units. In order to track the production of these species, it is also necessary to expand the number of radical distributions in the model to include P_0^{\bullet} (radicals of homopolymer BMA), and P_1^i (radicals ending in unit i that contain a single GMA unit) as well as P^i , radicals ending in unit i that contain two or more GMA units. Thus, the total number of distributed species tracked by the model increases from 3 to 8.

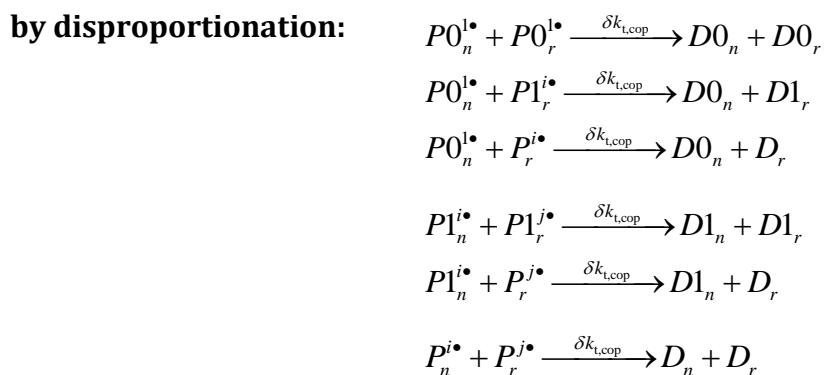
The set of mechanisms that needs to be considered also increases significantly, as summarized in Table 3-3. The radical fragment I^{\bullet} can react with BMA (M_1) to form P_0^{\bullet} , a new homopolymer chain of length 1, or it can react with GMA (M_2) to form $P_1^{2\bullet}$, a new chain of length 1 that already contains a single GMA unit. Propagation of

chain $PO_n^{1\bullet}$ with BMA leads to extension of the homopolymer chain, while addition of GMA leads to the formation of a GMA-ending radical of length $n+1$ that contains one GMA unit, $PI_{n+1}^{2\bullet}$. Similarly, propagation of chain $PI_n^{i\bullet}$ ($i=1$ or 2) with BMA keeps the resulting radical in the $P1$ distribution (product $PI_{n+1}^{1\bullet}$), while reaction with GMA moves the radical into the P distribution (product $P_{n+1}^{2\bullet}$ now containing two GMA units).

Care must be taken when considering the formation of dead polymer chains. For termination by disproportionation or chain transfer, the resulting dead polymer chain contains the same number of GMA units as the reacting radical; i.e., $PO_n^{1\bullet}$ is transformed to $D0_n$, $PI_n^{i\bullet}$ is transformed to $D1_n$ and $P_n^{i\bullet}$ is transformed to D_n . However, for termination by combination, the product molecule formed contains the total number of GMA units in both reacting radicals. Finally, it is important to track the identity of the new radical formed by chain transfer to BMA monomer (product radical $PO_1^{1\bullet}$) or by chain transfer to GMA monomer (product radical $PI_1^{2\bullet}$).

Table 3-3. Kinetic mechanisms of butyl methacrylate (BMA, 1) /glycidyl methacrylate (GMA, 2) copolymerization for expanded deterministic “counters” model. (See text for definition of radical and polymer distributions.)

Initiation**Propagation****Chain transfer to monomer****Chain transfer to solvent****Termination****by combination:**



Hybrid MC/Deterministic (PREDICI) The hybrid deterministic Monte Carlo algorithm¹⁴ implemented in PREDICI is based on the idea of splitting the underlying chemical master equation into the well-known kinetic rate equations coupled to properties better realized within a stochastic treatment (Equations (13,14) in ref¹⁴). The particular benefit of this splitting is that within the stochastic part one can make use of concentrations and reaction rates obtained by the deterministic method. This means that the rates as mentioned in the section about the pure MC method can be employed in a very exact manner without requiring too many realizations or molecules. As a consequence, the hybrid method performs a Gillespie-like algorithm in parallel to the deterministic method. However, there are some special aspects of this hybrid approach:

- The deterministic method proposes natural outer step lengths Δt and reaction rates valid for this time interval. The hybrid MC method then

performs all necessary steps (single step lengths as given in Equation (3.8)) within Δt to realize the number of events based on the given rates.

- Since the whole MC process works in parallel to *one* deterministic simulation, we do not want to repeat the treatment very often. Instead, a certain *constant* ensemble size of molecules is used in order to represent one population of polymer chains. This number is defined by the modeler. Since the computation time is mainly related to the ensemble size, it should be as small as possible but as large as necessary. Usually one will use smaller numbers for species with short lifetimes (i.e., radicals) and/or at a low concentration level and larger numbers for the long-living or product species. Due to the hybrid character of the method a direct error estimate is available (see Equation (30) in ref¹⁴), and thus adjustments of the ensemble sizes can easily be done for each distributed species. The following ensemble sizes for P^{\bullet} - $P^{2\bullet}$ - D have been used: 20-20-2000 and 100-100-5000. This choice leads to uniform errors of about 1-5%, based on the full number or weight chain length distributions, as shown in Figure 3-1 for the 20-20-2000 ensemble; the MW and composition averages considered (M_n , M_w , GMA fraction, etc.) are much more accurate. More details regarding error analysis may be found in the original description of the hybrid approach by Schütte and Wulkow.¹⁴
- A major task for the implementation of the hybrid method within the PREDICI context is its modularity. Whenever a special MC method is implemented for

a concrete and fixed model system, the underlying data structures as well as all properties under consideration can be created around the actual requirements. In a general program package it is necessary to define abstract properties related to the single steps forming a kinetic scheme. In the present implementation of PREDICI such an abstract property is called the “Monte Carlo index”; by operation of a single reaction this particular index of a chain is changed (usually increased by 1).

A chain of the hybrid MC method can also store all single events as a list e.g., leading to the sequence of monomer units along the backbone, or track topology (for branched systems). All reaction steps of PREDICI prepared for MC treatment can be assigned to one or more indexes. However, in this article we only make use of the basic property indices related to composition, with index 1 for incorporation of BMA and index 2 for GMA.

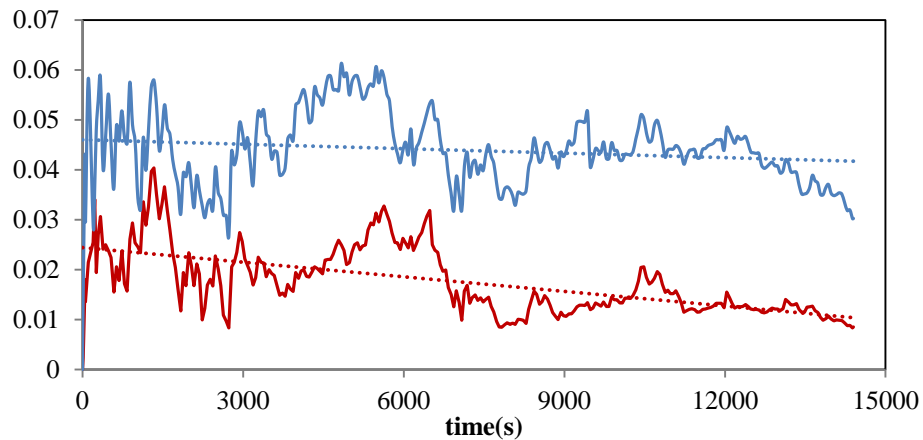


Figure 3-1. Time evolution of error determined by comparing deterministic and Monte Carlo-based dead polymer number (—) and weight (—) chain length distributions for an ensemble size of 2000 chains. The dotted lines are linear trend lines representing an averaged error.

3.4 Results and Discussion

The model described in Table 3-2 was run with the recipe specified in Table 3-1 using both the MC and basic deterministic formulations. The two models show exact agreement when examining output such as profiles of monomer concentrations, total radical concentration and number-average (M_n) and weight-average (M_w) polymer molecular weights (MWs), as shown in Figure 3-2. The noisiness of the radical concentration profile from the MC output results from the fact that the concentration (number) of radicals is the lowest of any species in the MC volume,

and thus shows the most fluctuation due to stochastic variation. However, the sample size selected ($n_{\text{rad}}=40$) is large enough to provide an accurate measure of reaction rate and MW averages, as seen in the negligible fluctuations relative to the mean values of these quantities, and the exact agreement with the deterministic model output.

The effect of sample size on the MC simulation output can also be seen in by examining the full polymer chain-length distribution (CLD), shown in Figure 3-3a, plotted using the customary logarithmic scale as would be measured by gel permeation chromatography (GPC). While the MC code provides an exact representation of the total number and weight of polymer chains in the system (and thus the M_n and M_w averages), the number of chains of a particular length is lower and hence more subject to fluctuations. Nonetheless, the agreement with the PREDICI output is excellent, as shown in Figure 3-3a. While the distribution shown is for the final polymer product, the evolution over the entire semibatch reaction period is tracked and can be examined, as done by Hamzehlou et al.⁸

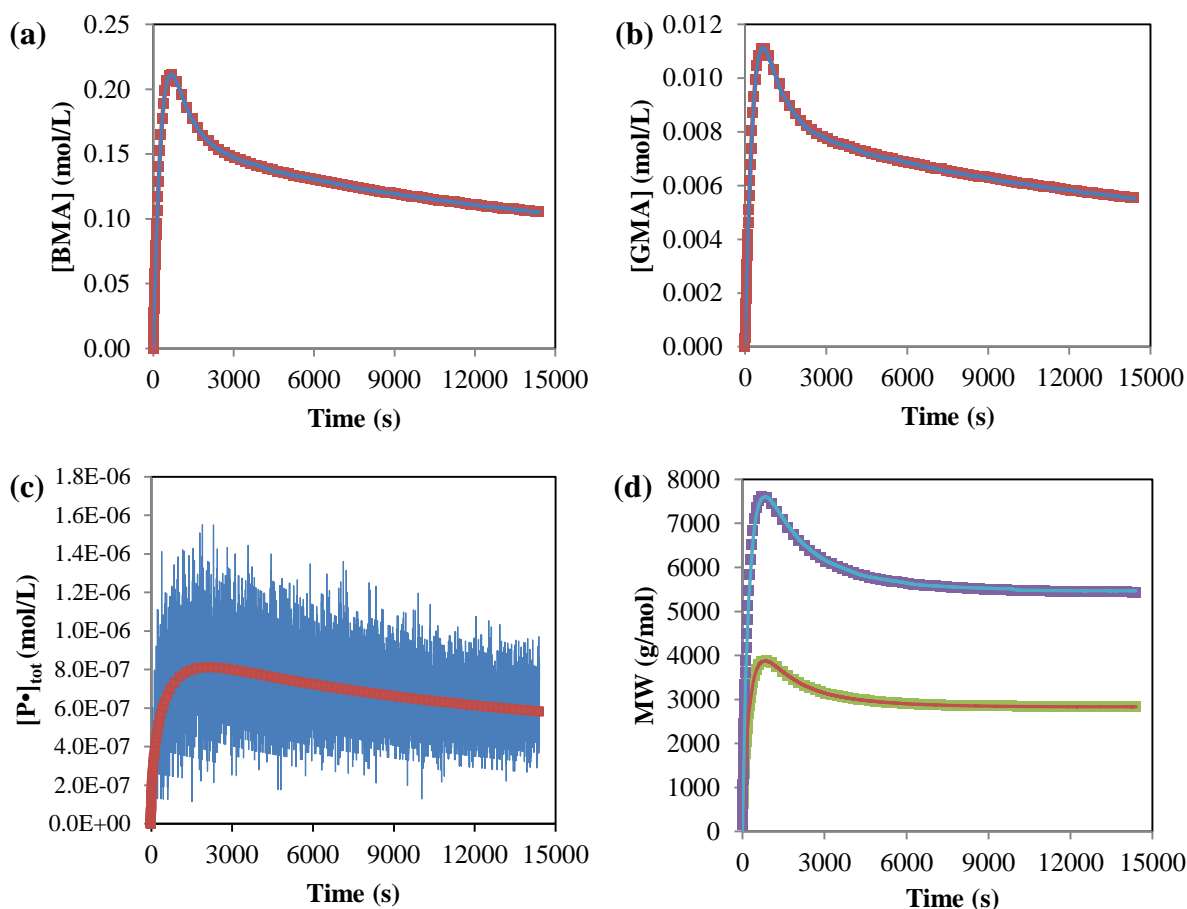


Figure 3-2. A comparison of standard output from the deterministic (■■■) and MC (—) simulations of the copolymerization system described in Tables 1 and 2: (a) [BMA] vs time, (b) [GMA] vs time, (c) total radical concentration vs time, (d) number-average (deterministic: ■■■ ; MC: —) and weight-average (deterministic: ■■■ ; MC —) MWs vs time.

The effect of MC sample size on simulated CLDs is shown in Figure 3-3b; Table 3-4 summarizes the corresponding simulation and CPU times required. Although the

concentration and average MW profiles are identical for simulations with n_{rad} values of 10 and greater, the output selected for presentation is calculated with $n_{\text{rad}}=40$. As the initial control volume (calculated according to the desired value of n_{rad} according to Equation (3.10)) is increased, the distribution becomes smoother and less susceptible to stochastic variation; however the simulation time also increases substantially. Since the control volume increases with time due to semibatch operation, the simulation also becomes slower towards the end of the feed period; Table 3-4 summarizes the final MC volume sizes for the simulations, also accounting for volume contraction during polymerization. As expected, the total time required for the PREDICI simulation is much reduced, in the order of seconds (10s) compared to over an hour for the MC simulation output shown in Figure 3-3a; the time required to set up and check the deterministic model is also significantly reduced. However, the extra information derived from the MC simulation not possible with the deterministic model is the distribution of the GMA units among the chains, as discussed below.

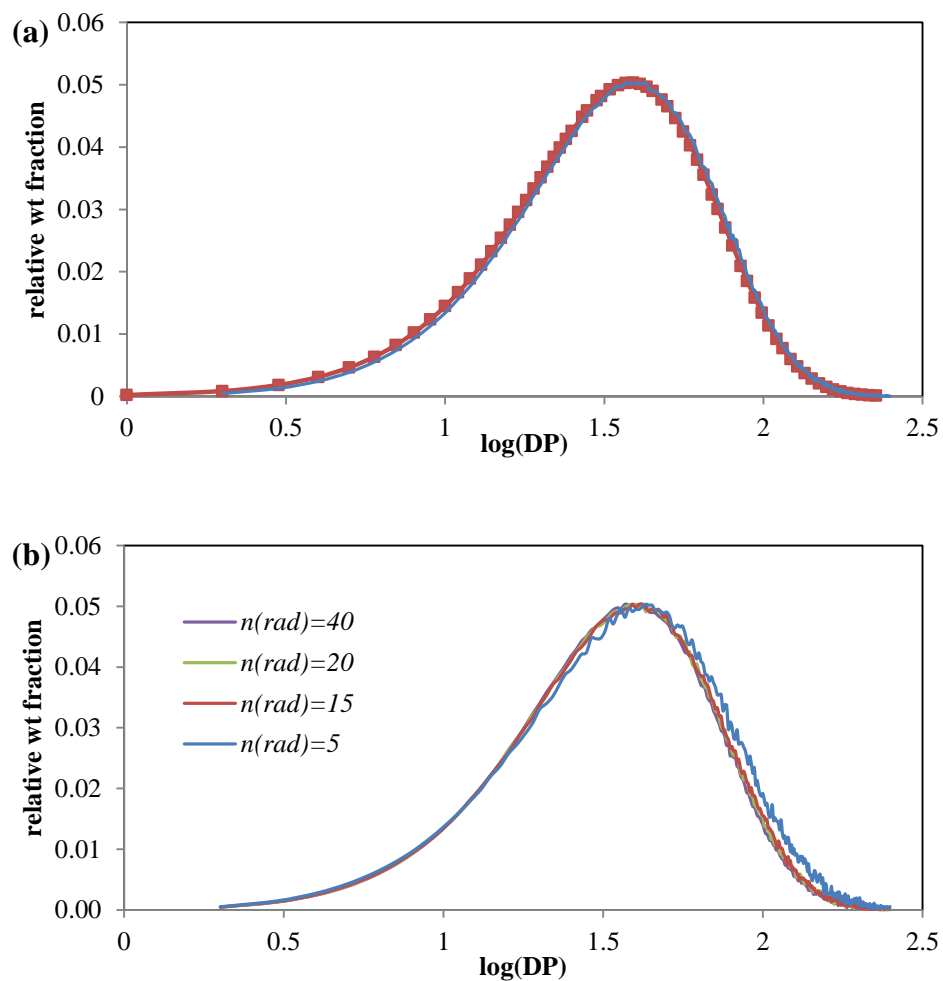


Figure 3-3. (a) A comparison of the final ($t=14400$ s) polymer chain-length distribution (GPC scale) from the deterministic (■■■) and MC (—) simulations of the copolymerization system described in Tables 1 and 2. (b) The effect of MC sample size on polymer GPC chain-length distributions.

Table 3-4. Initial and final MC volumes and simulation times for execution of MC code as a function of number of radicals.

Number of Radicals	$V_{MC}(0)$ (L)	$V_{MC}(14400s)$ (L)	Simulation time (min)	CPU time (hh:mm:ss)
5	3.070×10^{-18}	7.922×10^{-18}	9	0:08:37
10	6.140×10^{-18}	1.585×10^{-17}	17	0:18:15
15	9.211×10^{-18}	2.377×10^{-17}	25	0:44:37
20	1.228×10^{-17}	3.170×10^{-17}	33	1:19:29
25	1.535×10^{-17}	3.963×10^{-17}	41	2:03:17
30	1.842×10^{-17}	4.755×10^{-17}	49	2:55:39
40	2.456×10^{-17}	6.340×10^{-17}	66	4:05:33

The profiles shown in Figure 3-2 are typical of starved-feed operation: monomer concentrations remain low and polymer average MWs quickly attain constant values due to the fixed ratio of initiator to monomer that is fed.¹⁸ The feeding strategy minimizes copolymer composition drift, with the instantaneous composition of the polymer formed controlled by the monomer ratios in the feed. Thus, as shown in the kinetic MC study by Hamzehlou et al.,⁸ the composition of copolymer produced with a small amount (1 mol%) of functional monomer is kept uniform as a function of chain length and reaction time, in contrast to batch operation. In the example examined here, monomer reactivity ratios are unity such that monomer and copolymer composition control is perfect throughout the reaction with

$f_{m2}=F_{p2}=0.05$. In addition, with identical propagation rate coefficients assumed for GMA and BMA, the radical fraction is also constant at the same value:

$$f_{m2} = \frac{[\text{GMA}]}{[\text{GMA}] + [\text{BMA}]} = 0.05 = \frac{\sum_n [P_n^{2\bullet}]}{\sum_n [P_n^{1\bullet}] + \sum_n [P_n^{2\bullet}]} ; f_{m2} = F_{p2} \quad (3.12)$$

However, even with perfect control of overall copolymer composition, the low target chain length ($DP_n=20$) combined with the low GMA content in the copolymer ($F_{p2}=0.05$) leads to a significant population of chains without functionality. This quantity, as well as how the unfunctionalized (homopolymer) chains are distributed across the polymer MWD, cannot be followed using a conventional deterministic model, but is information easily tracked by the MC technique.

Figures 3-4 and 3-5 plot some of the information that can be processed from the MC output, which tracks the composition of every chain produced in the sample volume. Figure 3-4a shows the full CLD on a GPC scale, with the chains containing zero, one, and two GMA units shown as subdistributions. (The subdistributions are subject to stochastic noise at the tails of the distribution, leading to significant noise on the high MW-side when examined on the GPC scale.) Full information (i.e., distributions with three, four, etc. units per chain) is also available from the output, but has not been included in the plot for clarity. It is clear that a significant fraction of the chains produced do not contain the desired functionality (despite an average functionality of one unit per chain), and that most of the chains without functionality are, not

surprisingly, at the low MW side of the distribution. This latter result is seen more clearly in Figure 3-5a, which shows the fraction of chains containing zero, one, two, three, and more than three (four or greater) GMA units plotted as a linear function of chain length, as calculated from the MC output. As summarized in Table 3-5, the total number fraction of non-functional chains is quite high, approaching 50%, while the fraction of chains containing the desired single GMA unit is only 27%. The corresponding weight fraction of polymer without a GMA unit is lower at 25%, but still quite significant.

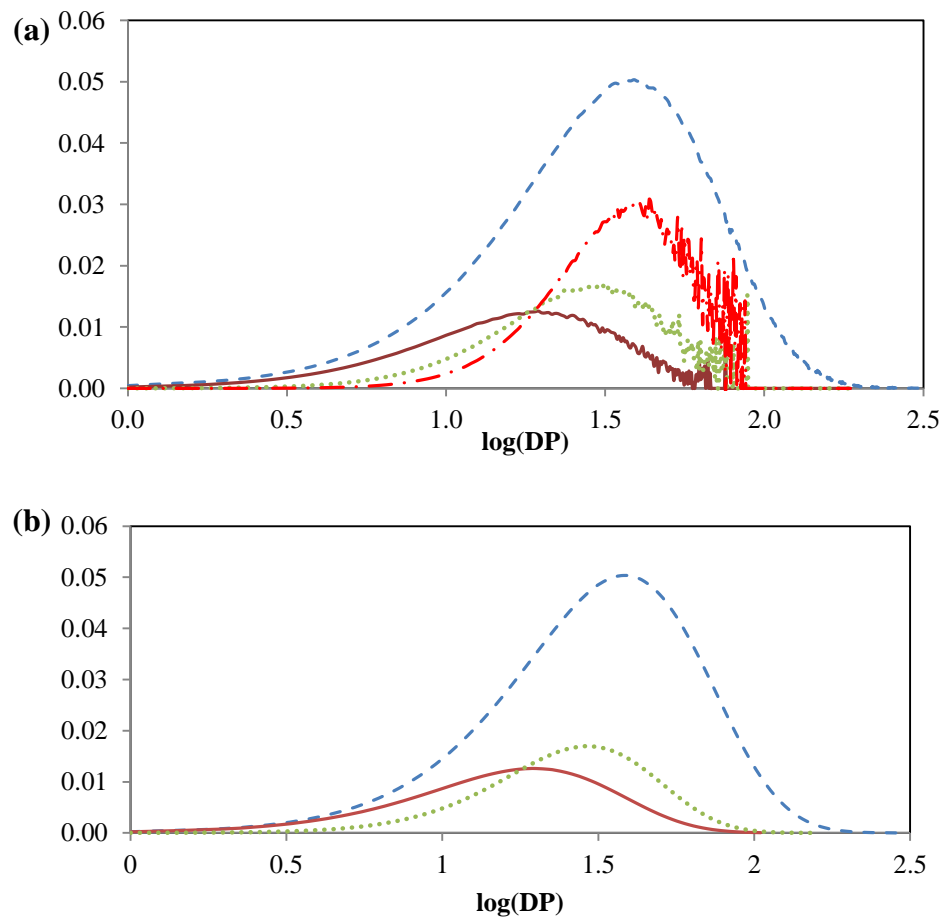


Figure 3-4. Full polymer chain-length distributions (GPC scale) (—) showing: (a) subdistributions of chains with zero GMA units (—), one GMA unit (····), and two GMA units (-·-·-) simulated by MC; (b) subdistributions of chains with zero GMA units (—) and one GMA unit (····) simulated by deterministic “counters” model.

Similar information can be obtained with the “counters” deterministic model, formulated to track the chains that contain zero and one GMA units, as well as those that contain two or more. With eight distributed species to track, the model takes slightly longer (90 sec) to run using PREDICI compared to the base deterministic model (10 sec, with three distributed species) but is much faster than execution of the MC code (66 min for $n_{\text{rad}}=40$). The standard output from the model (i.e., Figure 3-2 plots) matches that of the base deterministic model exactly. In addition, the model generates information regarding the distribution of GMA among the polymer chain, as shown in the plots of polymer CLD (Figure 3-4b) and fractional GMA composition as a function of chain length (Figure 3-5b), with output in agreement with the MC results. Table 3-5 compares the calculated distribution of GMA among the polymer chains from the two models. While the output from the deterministic model can be considered as exact, the MC sample size is large enough to provide excellent agreement.

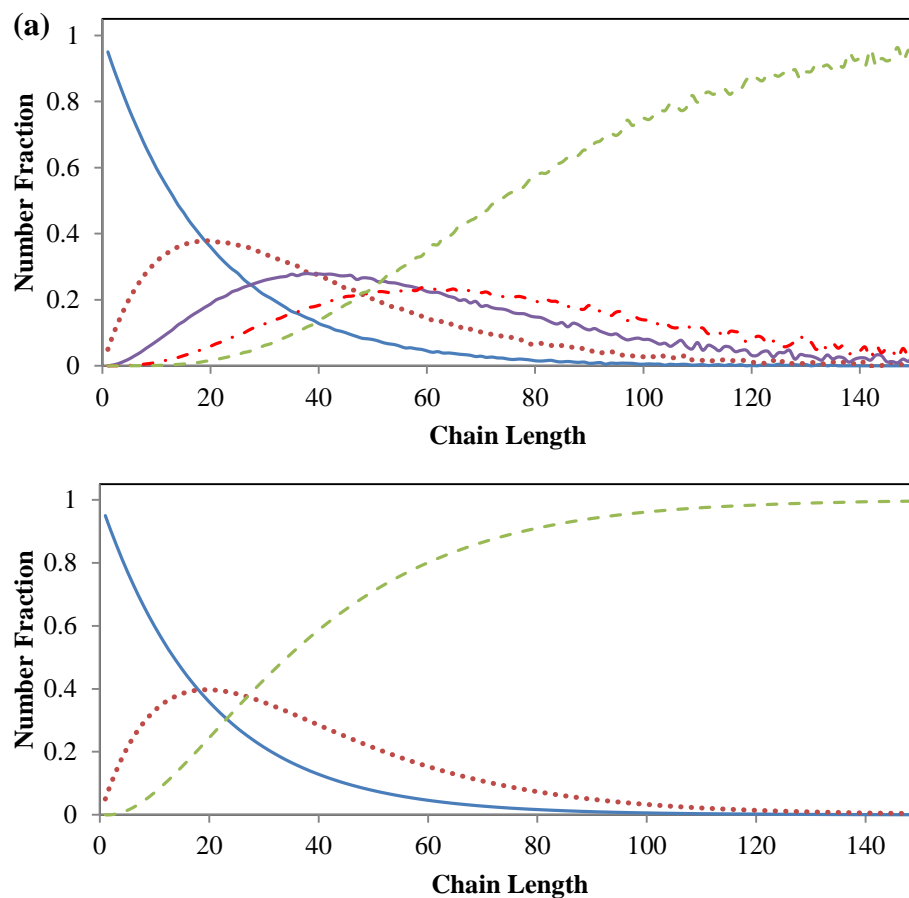


Figure 3-5. (a) Fraction of polymer molecules at each chain length with zero (—), one (.....), two (-.-.-), three (—), and four or more GMA units (---) calculated from MC simulation output. (b) Fraction of polymer molecules at each chain length with zero (—), one (.....), and two or more GMA units (---) simulated by deterministic “counters” model.

Table 3-5. Distribution of GMA units among polymer chains calculated by various modeling approaches for a perfectly controlled copolymerization system with $DP_n=20$ and $F_{GMA}=0.05$.

Model	Number fraction of polymer chains containing:				
	0 GMA	1 GMA	2 GMA	3 GMA	4 GMA
Monte Carlo ($n_{rad}=40$)	0.488	0.263	0.128	0.062	0.030
Deterministic Counters	0.486	0.264	<i>n.d.</i>	<i>n.d.</i>	<i>n.d.</i>
Hybrid PREDICI (2000 chains)	0.492	0.258	0.128	0.062	0.035
	0.484	0.262	0.129	0.064	0.031
	0.486	0.260	0.131	0.066	0.033
Hybrid PREDICI (5000 chains)	0.489	0.259	0.126	0.062	0.033
	0.493	0.259	0.125	0.059	0.033
	0.491	0.252	0.137	0.060	0.031

n.d.: not determined

So which modeling methodology can be considered as superior? The answer, not surprisingly, is that both approaches have strengths and weaknesses. While the simulation time for the deterministic counters model is significantly shorter, a certain level of expertise with model formulation and careful checking is required to expand the mechanistic set from Table 3-2 (base model) to Table 3-3 (expanded model) in PREDICI. While it is possible to extend the “counters” treatment to consider distributions with two, three, and more GMA units per chain, there will be a

concurrent increase in the set of mechanisms and the number of distributions to be tracked. This task will quickly rise in difficulty as the number of monomers and/or mechanisms (e.g., methacrylate depropagation, formation and reaction of midchain radicals in the presence of acrylate monomers¹⁸) in the base model increases. The resulting deterministic model, as formulated, provides an exact measure of the distributions of chains with zero or one unit per chain. While this output may be sufficient to develop new insights into the production of functional dispersant by free radical polymerization, it does not contain the details of the MC output which tracks the complete distribution of GMA units. This major advantage of the MC model is partially offset by the longer simulation time required to generate output, and the expertise required to formulate and check the computer code (usually against output generated by a deterministic model), including the influence of the simulation volume.

The “hybrid” concept of Schütte and Wulkow¹⁴ was developed to provide the benefits of both modeling approaches, combining the convenience and flexibility of model formulation and solution in PREDICI with the extra information provided by the MC approach. As described in that publication, the hybrid algorithm solves the full deterministic system using the Galerkin h-p approximation method for chain-length distributions and in parallel uses the MC technique to simulate single realizations of the stochastic process underlying chain growth. Thus, the basic model formulation in PREDICI (summarized by Table 3-1 and Table 3-2) can be used,

with a relatively small number of chains simulated stochastically in order to track the distribution of GMA units among the chains.

Example output from the hybrid model is shown in Figure 3-6 for a MC ensemble size of 2000 molecules for the dead polymer chains. Figure 3-6a plots the composition of each chain in the ensemble as a function of chain length. At longer chain lengths, the points converge toward the average GMA composition (0.05), but the composition of the shorter chains show much greater variability: while there are chains containing greater than average GMA incorporation, a significant number of chains containing no GMA units is also observed (points along the x-axis). The output can be sorted to provide a breakdown of the number chain-length distribution into chains containing 0, 1, 2, and 3 or more GMA units, as shown in Figure 3-6b; as for the MC simulation, full information (i.e., chains with three, four, etc. units per chain) is also available from the output, but is not included in the plot for clarity. The results are presented as a bar chart to illustrate the stochastic variability that results from the smaller sample size (2000 chains) used in the hybrid simulation. Note that species concentrations and average polymer MWs as well as the full MWD match exactly the previous output shown in Figures 3-2 and 3-3, as these quantities are calculated using the deterministic algorithm contained in PREDICI.

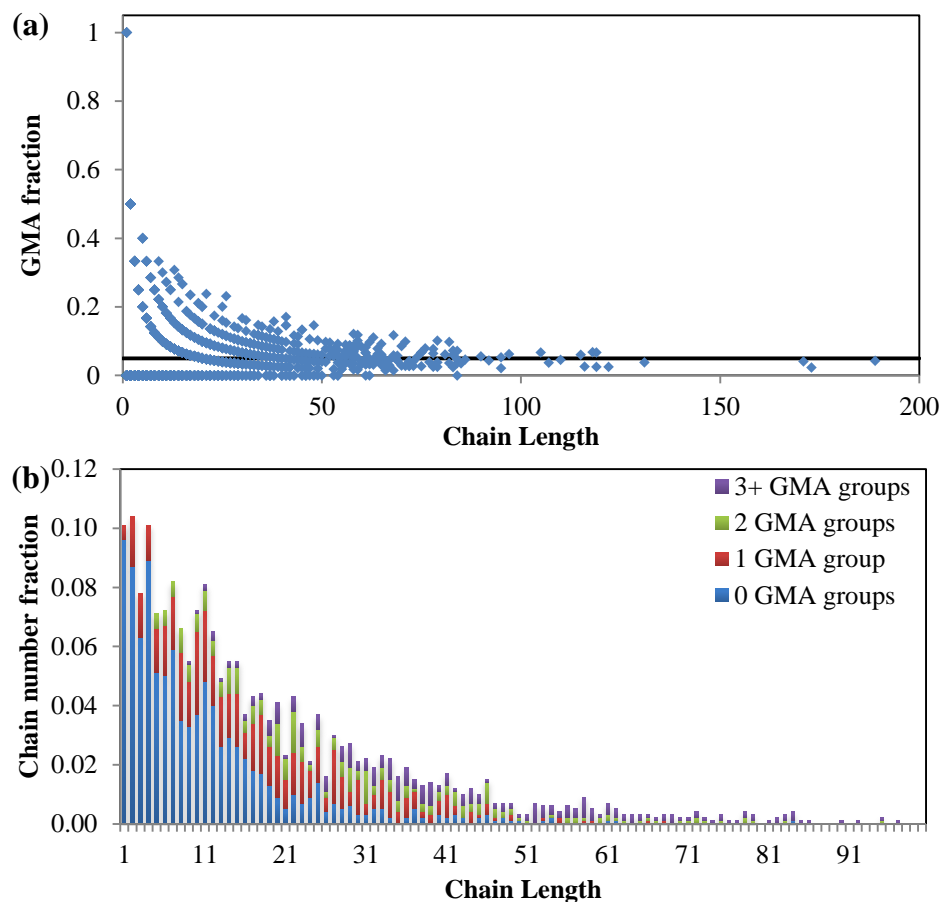


Figure 3-6. (a) GMA fraction in each chain and (b) overall number chain-length distribution, showing the chains with zero, one, two, and three or more GMA units, calculated for an ensemble size of 2000 molecules using the hybrid PREDICI model.

The fraction of total chains with a certain number of GMA units can also be plotted as a function of time, as compared to the deterministic “counters” model output (zero and one GMA units only) in Figure 3-7. The transients that occur over the first hour (e.g., lower value of total chains with zero GMA units) of the simulated reaction

are caused by the increased MW averages produced during that time period (see Figure 3-2d).

The selected outputs from the hybrid model (Figures 3-6 and 3-7) differ from those shown from the other modeling approaches (Figures 3-4 and 3-5) to provide another perspective on the distribution of the GMA functional groups. The numerical agreement between the methods is excellent, as summarized in Table 3-5 for the final polymer product (after 4 h). Output from three repeat runs using the hybrid model is included in the tabulated results to illustrate the stochastic variability for ensembles of 2000 (total simulation time of 10 min) and 5000 chains (total simulation time of 46 min). The results compare well with those generated from the other modeling approaches, with scatter in the third decimal place due to the smaller MC ensemble size.

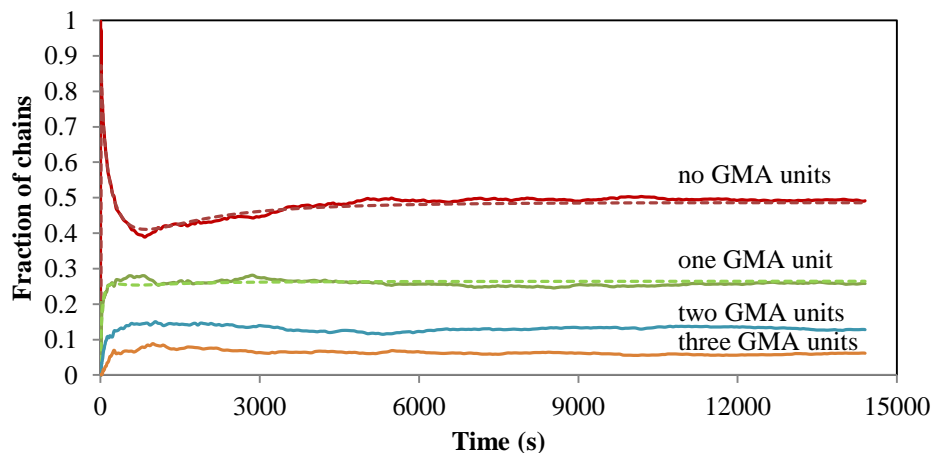


Figure 3-7. Fraction of total chains with zero, one, two, and three GMA units plotted against reaction time, calculated from simulation output from the hybrid (solid lines) and deterministic “counters” model (dotted lines, tracked for zero and one GMA units only).

3.5 Conclusions

Three modeling approaches have been used to simulate the distribution of GMA functional groups within the polymer molecular weight distribution produced by semibatch free-radical polymerization. Although perfect control of overall copolymer composition (5 mol% GMA incorporation) is achieved for this idealized case study, the low target chain length ($DP_n=20$) means that only a quarter of the chains produced have the desired functionality of one GMA unit per polymer molecule, with close to half of the chains produced containing no functional groups. This result from the MC formulation is compared to that from an extended

deterministic model implemented in PREDICI. The simulation time for the MC treatment (just over 1 h) was much greater than that of the deterministic “counters” model (1-2 min), although both models tracked the distributions of chains containing zero and one GMA units. While the MC simulation provides a full description of the 2D composition and chain length distributions not possible with the deterministic approach, care must be taken to ensure that the MC control volume is sufficiently large such that fluctuations in the concentrations of scarce species (in this case, the growing radicals) do not skew the results.

Both the MC and deterministic “counters” approaches require a certain level of expertise in model formulation, with the implementations verified against concentration and polymer MW profiles generated by a “basic” deterministic model. The new hybrid approach¹⁴ combines the basic model formulation and solution in PREDICI with the stochastic simulation of a small number of chains, providing a means to examine the distribution of a second quantity (comonomer composition in this case) as a function of chain length. The simulation times are between those of the deterministic and MC approaches and accurate results can be generated with no extra programming by the user. While it will not replace the utility or functionality of MC code written for specific applications, the hybrid formulation opens up the power of stochastic simulation to the casual model user.

References

- (1) T. Tadros, *Adv. Colloid Interface Sci.* **2009**, 147-148, 281.
- (2) K. E. J. Barrett, *Brit. Polym. J.* **1973**, 5, 259.
- (3) R. J. Barsotti, L. A. Lewin, C. Scopazzi, *US Patent 5763528*, **1998**.
- (4) W. H. Stockmayer, *J. Phys. Chem.* **1945**, 13, 199.
- (5) H. Tobita, *Polymer* **1998**, 39, 2367.
- (6) M. Al-Harthi, M. J. Khan, S. H. Abbasi, J. B. P. Soares, *Macromol. React. Eng.* **2009**, 3, 148.
- (7) P. H. M. Van Steenberge, D. R. D'hooge, Y. Wang, M. Zhong, M.-F. Reyniers, D. Konkolewicz, K. Matyjaszewski, G. B. Marin, *Macromolecules* **2012**, 45, 8519.
- (8) S. Hamzehlou, Y. Reyes, J. R. Leiza, *Macromol. React. Eng.* **2012**, 6, 319.
- (9) M. Wulkow, *Macromol. React. Eng.* **2008**, 2, 461.
- (10) E. Saldívar-Guerra, J. Bonilla, F. Becerril, G. Zacahua, M. Albores-Velasco, R. Alexander-Katz, L. Flores-Santos, L. Alexandrova, *Macromol. Theory Simul.* **2006**, 15, 163.
- (11) P. D. Iedema, M. Wulkow, H. C. J. Hoefsloot, *Macromolecules* **2000**, 33, 7173.
- (12) R. A. Hutchinson, *Macromol. Theory Simul.* **2001**, 10, 144.
- (13) P. Deuflhard, W. Huisinga, T. Jahnke, M. Wulkow, *SIAM J. Sci. Comput.* **2008**, 30, 2990.
- (14) C. Schütte, M. Wulkow, *Macromol. React. Eng.* **2010**, 4, 562.
- (15) A. Krallis, D. Meimaroglou, C. Kiparissides, *Chem. Eng. Sci.* **2008**, 63, 4342.
- (16) A. Brandolin, M. Asteasuain, *Macromol. Theory Simul.* **2013**, 22, 273.
- (17) W. Wang, M. C. Grady, R. A. Hutchinson, *Ind. Eng. Chem. Res.* **2009**, 48, 4810.
- (18) W. Wang, R. A. Hutchinson, *AIChE J.* **2011**, 57, 227.
- (19) D. T. Gillespie, *J. Phys. Chem.* **1977**, 81, 2340.
- (20) I. M. Maafa, J. B. P. Soares, A. Elkamel, *Macromol. React. Eng.* **2007**, 1, 364.

Chapter 4

Modeling of Branch Distribution in Chain Walking Polymerization: Combination of two Monte Carlo Techniques

4.1 Introduction

Demands for special properties have inspired scientists to form polymers with new chain architecture or topology that influences the rheology and end application of the polymer.¹ Dendritic polymers, a new category of polymer architecture including dendrimers and hyperbranched polymers, have been of interest to researchers for more than two decades now.¹⁻⁶

In comparison to traditional chain-growth polymerizations (e.g., free radical, ionic, cationic, coordination, group transfer), where the addition of the monomer usually occurs at the chain end to form linear polymers,⁷ during synthesis of dendritic polymers the catalyst center moves along the chain to form branched polymers. A three-dimensional spherical architecture is introduced in dendritic polymers, bringing advantages such as good stability, low melt/solution viscosity, and abundance of reactive sites or functionalities.^{2,8} In contrast to the dendrimers that need complicated multi-step synthesis, hyperbranched polymers, which have similar structure to dendritic architecture, are usually produced in more convenient single-step processes. This feature of hyperbranched polymers empowers mass

production and various industrial applications, from catalyst support to drug-delivery to coatings.⁸ Hyperbranched polyethylene synthesized with chain walking polymerization has potential application as shear-stable lubricant viscosity additives and polymer processing aids.⁹

In order to synthesize hyperbranched polymerization, a strategy for designing branched structures in polyolefin was introduced in 1999 by Guan et al. in which hyperbranched polyethylene was synthesized by a novel chain walking polymerization (CWP) system that uses Brookhart's Pd-diimine catalyst.¹⁰ Many developments have been since achieved to advance the synthesis of hyperbranched polymerization with Pd-diimine catalyst.¹¹⁻¹³ The branching density of polyethylenes produced using this catalyst (~100 branches/ 1000 carbons) is far higher than the branching density of LDPE synthesized via the high-temperature high-pressure radical processes.¹⁴

The catalyst controls the position of the next monomer insertion at any position along the chain, unlike other systems that introduce branching by monomer structure. The catalyst center, the metal site in this polymerization, walks randomly along the polymer chain. Therefore during propagation, the next monomer unit can be inserted anywhere along the polymer backbone instead of the chain end, as shown in Figure 4-1.¹⁵

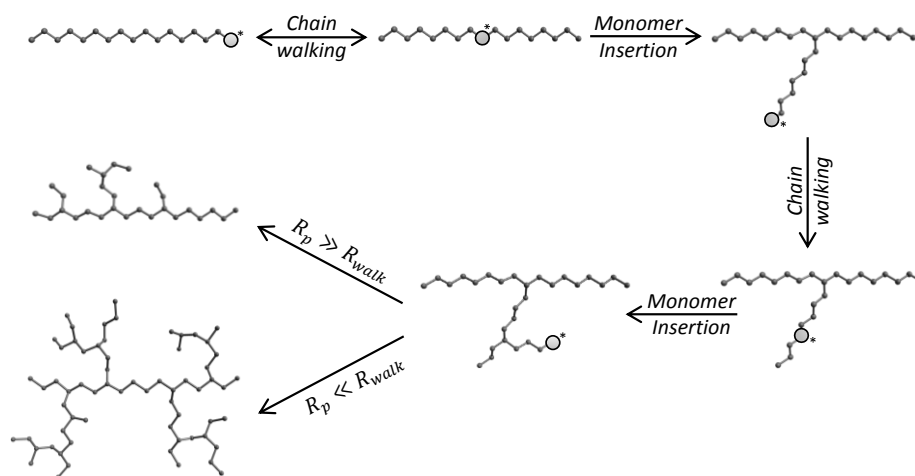


Figure 4-1. A schematic representation of ethylene polymerization with branch formation occurring after “chain walking” of the catalyst center along the chain. The two branched structures indicate the effect of changing polymerization conditions (redrawn from ref¹²).

The materials are generally produced by semibatch polymerization at constant ethylene pressure, as described by Ye et al.¹⁶ In brief, the polymerization at ethylene pressure of 1 atm is carried out in a 500 mL glass reactor. Dichloromethane (100 mL) is injected to the flame-dried reactor under protection of N_2 . After equilibrium for 10 min in an oil bath, a certain amount of catalyst stock solution is injected into the reactor in order to start polymerization. Polymerizations at 6.5 and 30 atm are conducted in a 1 L Autoclave stainless steel reactor. A mixture of dichloromethane (300 mL) and certain amount of catalyst stock solution are injected to the reactor under protection of N_2 . After 10 min of stirring and being heated to the reaction

temperature, the reactor is pressurized by ethylene gas to begin polymerization. The fluctuation of reactor pressure is eliminated by continuous feeding of ethylene gas from a cylinder.

Changing polymerization conditions, such as ethylene pressure, govern the polymer chain topology by shifting the competition between propagation and chain walking, two fundamental processes regulating the nonlinear chain growth. The difference in dependencies of ethylene concentration on chain propagation rate (R_p), where the rate reflects the combination of trapping and insertion elementary reactions, and chain walking rate (R_{walk}), makes ethylene pressure an easily-adjustable parameter to mediate the two competing rates.⁹ Studies show that the R_p is basically independent of ethylene pressure and the R_{walk} is, in contrast, an inverse first-order function of ethylene pressure (P_e).^{10,17,18} Therefore, a high branching density with extensive branch-on-branch structure is achieved in low pressure in which R_{walk} is much faster than R_p . On the other hand, linear polymers with mainly short branches will be synthesized in high pressure when R_p is notably greater than R_{walk} .⁹ Consequently, an increase in ethylene pressure means an increased intrinsic viscosity at equal molecular weights to those polymers synthesized at lower pressure.^{10,19}

In addition to chain walking and propagation (also known as insertion) reactions, Johnson et al. proposed two other basic mechanisms.¹⁴ Absorption of the ethylene molecule on the catalyst, called association or trapping, creates a condition where

insertion can take place. In this situation, chain walking cannot happen and the catalyst site is considered to be in the “resting state”. The absorbed monomer has a possibility of leaving the metal site by dissociation, causing the “active state” of the catalyst to be resumed, in which chain walking is probable to take place.

Thus, these four steps are occurring during formation of a hyperbranched chain. After the monomer dissociates from resting state S_1 , the metal site walks along the chain (or branches on the chain) through β -hydride elimination, W_1, W_2, W_3, \dots (see Figure 4-2). This step can be repeated several times until the catalyst associates with another ethylene molecule, resulting in a new resting state S_2 . By insertion of the ethylene molecule, a new branch is created. As mentioned previously, the chain walking distance (the number of carbons the metal site walks through before insertion of the next monomer) is affected by ethylene pressure, P_e . At higher P_e , trapping occurs at a faster rate, and the average walking distance is comparatively short. At low P_e , the catalyst may walk through many carbons before inserting new monomer, forming branch-on-branch topology.¹⁰

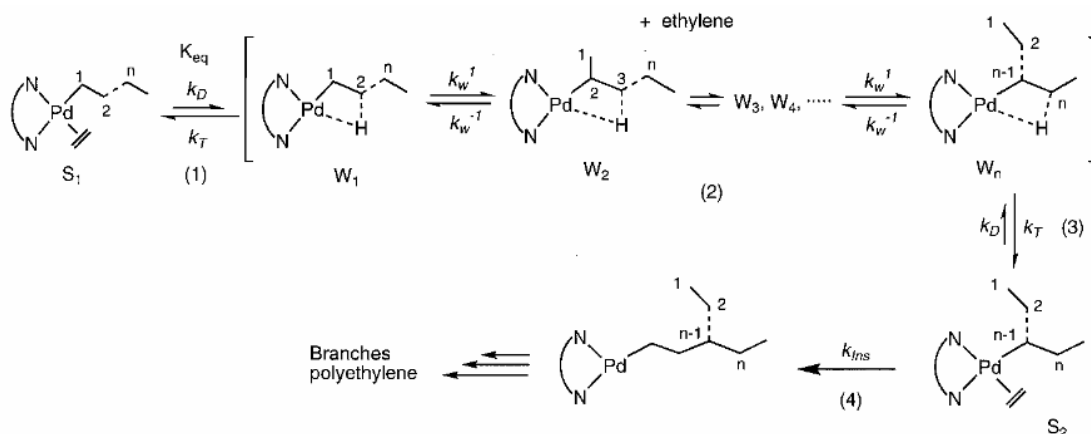


Figure 4-2. Mechanistic model for ethylene polymerization with Pd-diimine catalyst. Kinetics are (1) dissociation of monomer, (2) chain walking, (3) trapping of monomer (association), and (4) insertion of monomer. K_{eq} ($= \frac{k_D}{k_T}$) is the equilibrium rate coefficient for trapping/dissociation, and k_{ins} and k_w are the rate coefficient for insertion, and chain walking (1 for forward and -1 for backward chain walking), respectively (adopted from ref ¹²).

Numerous Monte Carlo studies have been done for branched molecules such as dendrimers and hyperbranched polymers,²⁰⁻²³ focused mainly on conformational properties e.g., radius of gyration. They have investigated the effect of different topological parameters such as generation (branch level) as a function of spacer length (linear section of the molecule) on the radius of gyration, or solvent type on dendritic molecule size and shape. The effect of branching topology on the branch distribution is, however, still not perfectly studied. The simulation study of randomly branched molecules developed by Chen et al.²⁴ illustrates the topology

and conformational behavior of hyperbranched polymers as well as the effect of changing reaction fixed probabilities on branch distribution. While the study successfully describes the effect of branching on polymer conformation and the radius of gyration (R_g), it does not consider two important factors: the time evolution of structure that is crucial for polymerizations in which conditions (e.g., pressure) vary with time; and reaction rates of the events in the system. Gillespie's algorithm, which is a well-known Monte Carlo method for tracking the reaction time in coupled chemical reactions, can be merged with Escobedo's algorithm developed by Chen et al., leading to a more comprehensive representation of hyperbranched polymerization by taking into account all reaction rates and related rate coefficients, as well as the polymerization time.

4.2 Methodology

4.2.1 Escobedo's Algorithm

A dynamic kinetic Monte Carlo model of Chain Walking Polymerization has been developed in order to simulate polymerization of ethylene with Pd-catalyst, as investigated experimentally in Ye's lab at Laurentian University. The model is a combination of algorithms developed by Chen et al.²⁴ (Escobedo's algorithm) and the Gillespie's algorithm for coupled chemical reactions.

In Escobedo's algorithm, intermolecular and intramolecular interactions of a growing polymer are neglected. The competition between chain walking and ethylene trapping at an active state is considered as an input parameter, the probability of chain walking P_w . As the schematic flowchart Figure 4-3 shows, a uniformly random number ($ran1$) is generated to choose between chain walking and trapping reactions, the two competing events for a chain in active state. If $ran1 < P_w$, chain walking will happen, otherwise the chain converts to the resting state by trapping an ethylene molecule at the metal site. P_w is a function of ethylene pressure, P_e , since the trapping reaction rate is first order based on ethylene concentration (ethylene pressure). The following equation expresses the relation between P_w and P_e :

$$P_w = \frac{R_w}{R_w + R_T} = \frac{R_w}{R_w + k_t P_e} \quad (4.1)$$

where R_w , R_T , and k_t are the rate of chain walking, the rate of ethylene trapping, and the rate coefficient for ethylene trapping (expressed with respect to ethylene pressure), respectively.

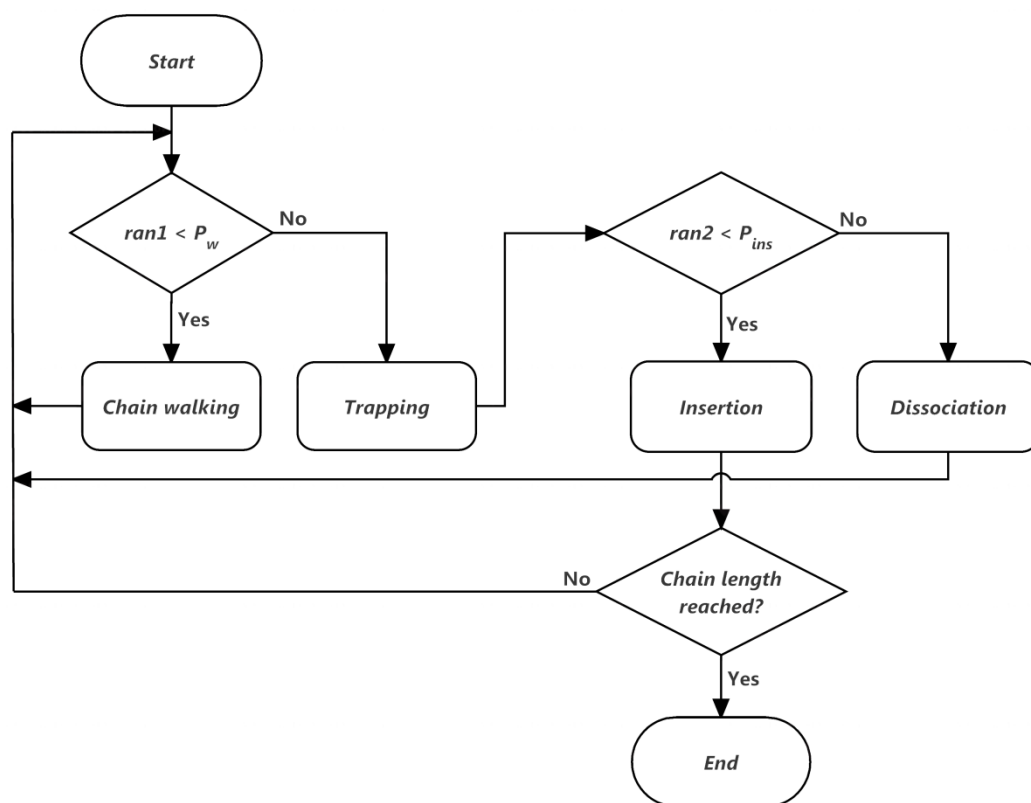


Figure 4-3. Flowchart showing the order of events in MC simulation of Pd-diimine-catalyzed chain walking polymerization, Escobedo's algorithm.²⁴

There is also a competition between insertion and dissociation after the catalyst has trapped a monomer. Therefore a second parameter, P_{ins} , is introduced to account for the probability of insertion. A new random number ($ran2$) is compared with P_{ins} ; if $ran2 < P_{ins}$, then the trapped ethylene will be inserted into the chain, otherwise it will dissociate from the metal site to convert the chain back to the resting state.

Due to steric effects, Chen et al. assumed that the probability of insertion at chain ends, P_{ins}^{end} , must be higher than the probability of insertion at inner points, P_{ins}^{inner} ; having more mobility and consequently exploring more space, segments at a chain end have a higher chance of insertion compared to the inner segments. Therefore, it is necessary to distinguish the probability of insertion at the chain end from that at the inner points.

In addition, steric effects cause more difficulty in insertion of a monomer when the insertion occurs closer to a branch point. To consider this effect, the parameter, f , was introduced by Chen et al. as a correction factor for P_{ins} :

$$f = 1 - e^{-x} \quad (4.2)$$

Therefore the adjusted insertion probability is a function of distance from a branch point:

$$P'_{ins} = P_{ins} \times f \quad (4.3)$$

where x is the number of sites between the insertion point and the closest branch point. If the insertion point is at or adjacent to the branch point (i.e., $x = 0$), f will be 0 and subsequently no insertion will happen. Experimental observation from ^{13}C NMR studies of polymerization catalyzed by Ni catalyst supports that no adjacent branching occurs, and also that no quaternary carbons are observed.^{25,26} f increases exponentially to 1 when x increases from 0 to 4, so practically f is 1 for $x \geq 4$. The factor f applies to both probabilities of insertion (inner or end), but an additional

factor must also be considered for probability of insertion at the carbon adjacent to the chain end. The methyl bias factor, m , has been introduced in simulations of Ni-catalyzed polymerization, as it has been experimentally observed that methyl branches predominate over longer branches.²⁷ This predominance of methyl branches indicates a shift in the insertion-dissociation equilibrium toward insertion when the catalyst center is on the adjacent carbon to the chain end. In this situation, the insertion probability is adjusted as:

$$P_{ins}^{inner'} = m \times P_{ins}^{inner}, \quad m > 1 \quad (4.4)$$

Chen et al. adjusted the simulation parameters (P_w , P_{ins}^{end} , P_{ins}^{inner} , and m) in order to match experimental short chain branch distributions. Branch distributions are measured experimentally by ¹³C NMR, which cannot distinguish branch lengths if they are longer than 6C units. The parameters for the simulation were adjusted until the simulated short chain branch distribution was consistent with experimental results, as summarized in Table 4-1:

Table 4-1. Short chain branch distribution for the best set of simulation parameters of Escobedo’s algorithm, and experimental branch distribution. Me, methyl; Et, ethyl; Pr, propyl; Bu, butyl; Am, amyl; Hx+, hexyl and longer branches.²⁴

Entry	Simulation Parameters				Number of branches per 1000 CH ₂						
	P_w	P_{ins}^{end}	P_{ins}^{inner}	m	Me	Et	Pr	Bu	Am	Hx+	Total
1	Experimental results ²⁸				37.0	25.0	3.0	12.0	1.0	37.0	115.0
2	0.9	0.9	0.02	3	33.4	26.4	1.8	15.4	1.4	34.4	112.6

4.2.2 Implemented Gillespie’s Algorithm

In order to track structure as a function of polymerization time, Escobedo’s algorithm as described above is combined in this work with Gillespie’s algorithm. Gillespie’s algorithm requires the absolute reaction rates of all events in the system, unlike Escobedo’s method which is based on relative rates. While chain transfer also occurs in some CWP systems,²⁹ the mechanism is omitted from the current implementation as it has no influence on the chain topology.¹⁰ Table 4-2 lists all the reactions used by Chen et al. and the respective reaction rate expressions.

Among the four reaction rates in the system, the insertion rate changes dependent upon the position of the catalyst center on the chain. For example, the probability of insertion for a chain in the resting state, Pd_R , is different when the catalyst center is

located at the adjacent carbon to the chain end that is 2 carbons away from the nearest branch, $Pd_R^{adj,x=2}$, than compared to when insertion takes place at the catalyst center adjacent to the end carbon with $x \geq 3$, $Pd_R^{adj,x \geq 4}$. Thus, the insertion event is split into 12 reactions, covering all of the possible insertion situations. These 12 insertion reactions are organized in three categories: insertions at the chain end, insertions at the adjacent carbon to the chain end, and insertions at other inner segments. The rates of chain walking, trapping, and monomer dissociation, on the other hand, are not affected by the position of the catalyst center; if chain walking happens to a chain in the active state, Pd_A will change to Pd_A^* to indicate that the position of the catalyst center has shifted; x is not shown as part of the mechanism, although is tracked internally. The direction of chain walking is also chosen randomly.

Table 4-2. Kinetic mechanism of ethylene polymerization with Pd-diimine catalyst. Catalyst center is moved in the species specified with asterisk.

Chain walking		
1	$Pd_A \xrightarrow{k_w} Pd_A^*$	$R_w = k_w[Pd_A]$
Insertion		
2,3,4	$Pd_R^{end,x=i} \xrightarrow{fk_{ins}^{end}} Pd_A, \quad i = 1,2,3.$	$R_{ins}^{end,x=i} = fk_{ins}^{end} [Pd_R^{end,x=i}]$
5	$Pd_R^{end,x \geq 4} \xrightarrow{k_{ins}^{end}} Pd_A$	$R_{ins}^{end,x \geq 4} = k_{ins}^{end} [Pd_R^{end,x \geq 4}]$
6,7,8	$Pd_R^{adj,x=i} \xrightarrow{mfk_{ins}^{inner}} Pd_A, \quad i = 1,2,3.$	$R_{ins}^{adj,x=i} = fmk_{ins}^{inner} [Pd_R^{adj,x=i}]$
9	$Pd_R^{adj,x \geq 4} \xrightarrow{mk_{ins}^{inner}} Pd_A$	$R_{ins}^{adj,x \geq 4} = mk_{ins}^{inner} [Pd_R^{adj,x \geq 4}]$
10,11,12	$Pd_R^{x=i} \xrightarrow{k_{ins}^{inner}} Pd_A, \quad i = 1,2,3.$	$R_{ins}^{x=i} = fk_{ins}^{inner} [Pd_R^{x=i}]$
13	$Pd_R^{x \geq 4} \xrightarrow{k_{ins}^{inner}} Pd_A$	$R_{ins}^{x \geq 4} = k_{ins}^{inner} [Pd_R^{x \geq 4}]$
Dissociation		
14	$Pd_R \xrightarrow{k_D} Pd_A + M$	$R_D = k_D[Pd_R]$
Trapping		
15	$Pd_A + M \xrightarrow{k_T} Pd_R$	$R_T = k_T[Pd_A][M]$

Initial estimates for the possible range of the rate coefficients were provided through email correspondence with Dr. Zhibin Ye, as summarized in Table 4-3.

Table 4-3. Values of ethylene chain walking polymerization rate coefficients reported from Dr. Zhibin Ye's lab.

Rate coefficient (unit)	Range or value
k_{ins} (s ⁻¹)	0.1 – 2
k_D (s ⁻¹)	20
$K_{eq} = \frac{k_D}{k_T}$ (mol/L)	10 ⁻³ – 10 ⁻⁴
k_w (s ⁻¹)	10 ⁴ – 10 ⁵

In Escobedo's algorithm, P_{ins}^{inner} and P_{ins}^{end} are adjusted to match available experimental data.²⁴ To reduce the number of parameters that are independently varied to match experimental results, as well as to utilize the probability values introduced by Chen et al. as variables, a cascade procedure for varying parameter values has been established. The basic idea is to specify k_{ins}^{end} and K_{eq} ($= k_D/k_T$), and then calculate k_D and k_w from Escobedo's probabilities.

$$P_{ins}^{end} = \frac{k_{ins}^{end}}{k_{ins}^{end} + k_D} \quad (4.5)$$

Given k_{ins}^{end} and P_{ins}^{end} , k_D is calculated from Equation (4.5). Then, k_{ins}^{inner} is computed based on a similar equation to Equation (4.1):

$$k_{ins}^{inner} = k_D \times \frac{P_{ins}^{inner}}{1 - P_{ins}^{inner}} \quad (4.6)$$

After calculating k_T with the given value of K_{eq} , k_w is calculated using the value of ethylene concentration estimated as a function of ethylene pressure (as described later):

$$k_w = k_T[M] \times \frac{P_w}{1 - P_w} \quad (4.7)$$

Hence, the cascade calculation provides values for k_D , k_w , k_{ins}^{inner} , and k_T by using input values of k_{ins}^{end} , K_{eq} , P_{ins}^{end} , P_{ins}^{inner} , P_w , and $[M]$. Once k_w is fixed, the probability of chain walking will change as P_e varies.

As described above, the classic MC algorithm introduced by Gillespie³⁰ has been combined with Escobedo's algorithm. Thus, macroscopic, or experimental, reaction rate coefficients (k^{exp}) must be converted to microscopic reaction rate coefficients (k^{MC}) according to the following, with V^{MC} the MC reaction control volume, calculated as discussed later.

$$k^{MC} = k^{exp} \quad (4.8)$$

for first order reaction, and

$$k^{MC} = \frac{k^{exp}}{V^{MC} N_A} \quad (4.9)$$

for bimolecular reactions between different species.

The MC rate of the ν th reaction, R_ν , is given by:

$$R_\nu = k^{MC} C_\nu \quad (4.10)$$

where C_ν is the number of possible combinations between reactants engaged in the ν th reaction. For example, C_ν for the trapping reaction from Table 4-2 is calculated as:

$$C_{15} = \binom{n_{PdR}}{1} \binom{n_M}{1} = n_{PdR} \times n_M \quad (4.11)$$

where n_{PdR} and n_M are the numbers of chains at resting state and monomer molecules in the system, respectively. The probability of each reaction, P_ν , is defined as:

$$P_\nu = \frac{R_\nu}{\sum_{\nu=1}^{N_{rxn}} R_\nu} \quad (4.12)$$

where N_{rxn} is the total number of reactions in the polymerization mechanistic set summarized in Table 4-2. Two uniformly distributed random numbers, r_1 and r_2 , are generated to choose the reaction that takes place at the polymerization time and the time step, respectively. Reaction μ happens if the following inequality is satisfied:

$$\sum_{\nu=1}^{\mu-1} P_\nu < r_1 \leq \sum_{\nu=1}^{\mu} P_\nu \quad (4.13)$$

with the time step, τ , computed as:

$$\tau = \frac{1}{\sum_{\nu=1}^{\mu} R_\nu} \ln \left(\frac{1}{r_2} \right) \quad (4.14)$$

k_T is the only rate coefficient corresponding to trapping second order reaction.

Therefore:

$$k_T^{MC} = \frac{k_T^{exp}}{V^{MC} N_A} \quad (4.15)$$

k_t and k_T both represent the rate coefficient of trapping reaction. For Gillespie's algorithm, monomer concentration, $[M]$, is needed (hence rate is proportional to $k_T [M]$), whereas Chen et al. expressed ethylene concentration in term of gas phase ethylene pressure, P_e . Therefore, we need to convert P_e to monomer concentration according to:

$$k_t = \frac{k_T^{exp} [M]}{P_e} \quad (4.16)$$

The relationship between $[M]$ and P_e is captured according to Raoult's law, as described later.

In order to calculate the MC control volume, V^{MC} , the number of catalyst molecules in the MC system, n_{Pd} , is set to obtain a sufficient "sample" of the polymer chains, since $n_{Pd} = n_{polymer}$. Then the ratio of n_{Pd}/n_{Pd}^{exp} is fixed based on experimental conditions,

$$conversion\ ratio = n_{Pd}/n_{Pd}^{exp} \quad (4.17)$$

where n_{Pd}^{exp} is the number of catalysts molecules in the actual experiment ($n_{Pd}^{exp} = mol\ Pd \times N_A$). Therefore, the sample volume size (V^{MC}) would be:

$$V^{MC} = V^{exp} \times \text{conversion ratio} \quad (4.18)$$

with V^{exp} the volume of experimental system. The volume expansion or reduction due to constant addition of monomer and propagation of the chains is not considered in this model, since the amount of dissolved polymer in the solvent is kept low and has a negligible impact on the volume.

A vapour liquid equilibrium relationship is needed in order to estimate the dissolved amount of monomer in the liquid phase from the ethylene pressure in the gas phase. In this study, Raoult's law is an applicable choice because the operational condition of the system is at low to moderate pressures (1 to 30 atm) and low temperatures (0 to 35°C) such that the liquid phase can be considered as an ideal solution³¹ due to the low solubility of ethylene in the solvent (e.g., chlorobenzene). It is assumed that the vapour phase contains purely ethylene gas, therefore the method only demands for the saturation vapour pressure of ethylene at the operating temperature, regardless of solvent type. Vapour pressure of ethylene is calculated from an equation fitted to experimental data by Michels and Wassenaar.³² If y_{gas} and P_{gas}^{sat} are respectively mole fraction of ethylene in the gas phase and vapour pressure of ethylene, therefore the mole fraction of ethylene, x_{gas} , in the liquid phase is calculated as follows, leading to the value of monomer concentration used in Equation (4.16):

$$x_{gas} = \frac{y_{gas} P_e}{P_{gas}^{sat}} \quad (4.19)$$

The overall simulation algorithm proceeds as follows: First the Gillespie's probabilities are calculated based on all reaction rates and the number of each species in the system. Chains in the active and resting states are considered as distinguished species in order to calculate reaction rates. Similarly, chains with the same catalyst center condition (e.g., catalyst center on adjacent carbon to the chain end) are also treated as the same species. Three uniformly random numbers are generated to select the next reaction, to compute the time interval, and to choose a chain among eligible chains for the selected reaction. After the randomly selected reaction takes place, the affected molecule numbers as well as the topology information of the chosen chain are updated. While the stop condition (which can be either the polymerization end time or the specific average chain length) is not satisfied, the loop continues.

4.3 Results and Discussion

A sensitivity analysis was done before adjusting the input parameters to match available experimental data. K_{eq} , k_{ins}^{end} , P_{ins}^{end} , P_{ins}^{inner} , P_w , and m were varied systematically to examine their effect on branch distribution, average chain length, and total number of branches; during the analysis of a factor, all other parameters were fixed, since the input parameters are independent of each other. Three

simulation end times were selected to find the effect of the changing parameter at early, middle, and final stages of polymerization.

4.3.1 Sensitivity Analysis: Average Chain Length

The effect of the parameters on average chain length is summarized in Figure 4-4, with output calculated for reaction times of 1000, 3000, 5000, and 7000 s. Longer polymerization duration increases the average chain length for all parameter values, as there is no termination taking place in this system. An increase in k_{ins}^{end} (that consequently leads to increased k_D) or P_{ins}^{inner} (see Equation (4.6)), results in longer average chain lengths due to the increased rate of monomer insertion. P_{ins}^{end} has a reverse relation to k_D : higher P_{ins}^{end} causes a decrease in k_D (Equation (4.5)) such that the dissociation of the monomer is more probable, decreasing the average chain length of the final polymer.

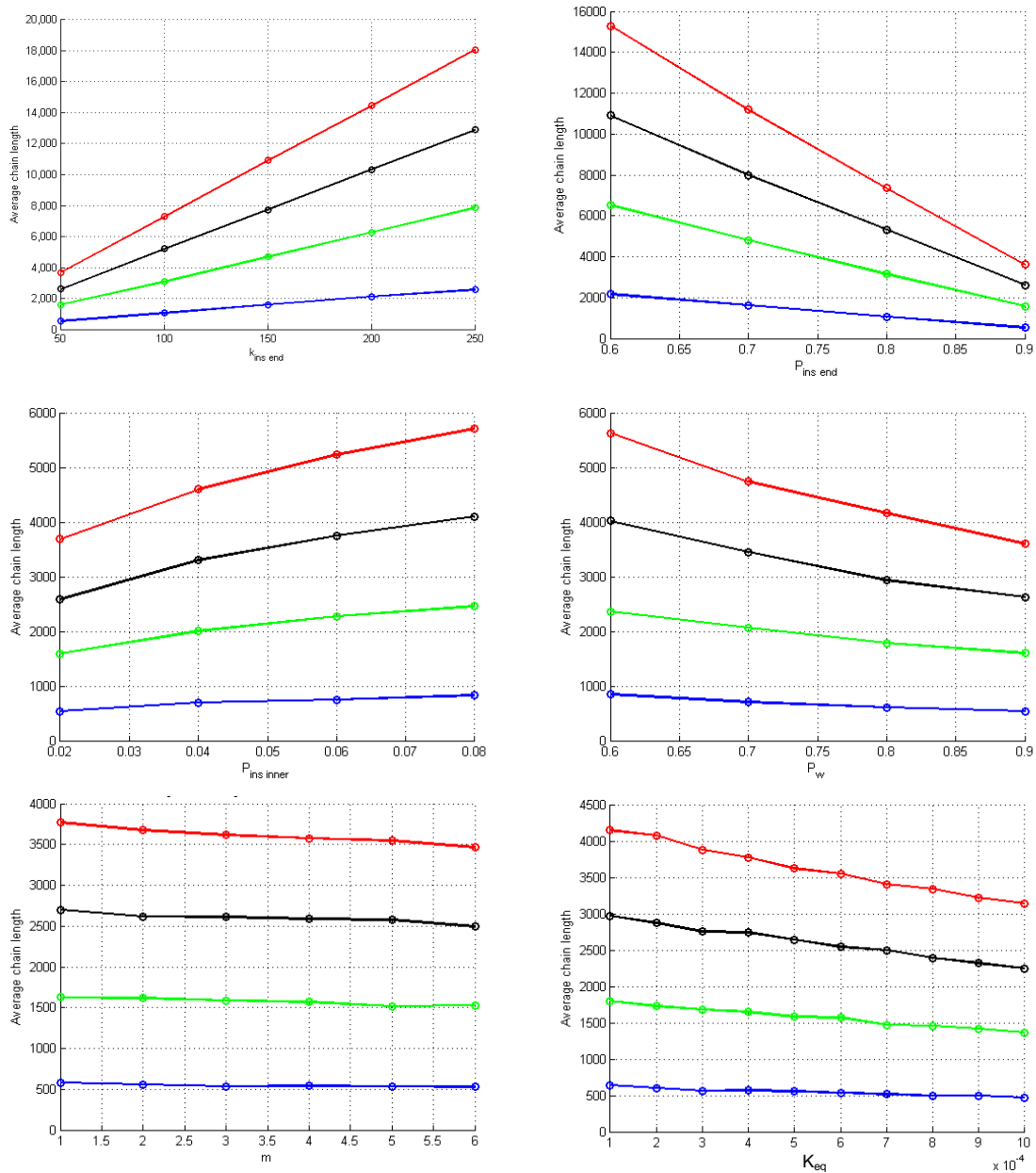


Figure 4-4. Effect of varying values of k_{ins}^{end} , P_{ins}^{end} , P_{ins}^{inner} , P_w , m , and K_{eq} on average chain length for reaction times of 1000s (—), 3000s (—), 5000s (—), and 7000s (—).

An increased value of P_w means higher k_w (Equation (4.7)) and thus more chain walking events and more branching, leading to shorter average chain lengths (decreased monomer insertion) for the same reaction time. As methyl branches are the shortest alkyl group, an increase in its population (resulting from an increased value of m) does not change average chain length significantly. An increase in K_{eq} when k_D is fixed leads to a smaller value for k_T that leads to a decrease in average chain length. This decline, however, is not very significant due to large difference in the magnitudes of k_D and k_T .

4.3.2 Sensitivity Analysis: Total Number of Branches

The effect of the input parameters on the total number of branches (calculated per 1000 C-atoms) is shown as Figure 4-5. The values of k_{ins}^{end} and K_{eq} do not effect either the total number of branches or the branch distribution, as these quantities are only affected by the relative probability parameters defined by Chen et al. The branching density increases with increasing values of P_{ins}^{inner} , P_w , and m . An increase in P_w indicates that chain walking takes place more often between insertions, resulting in more branches. The higher probability of monomer addition at inner segments of the chain, a consequence of an increase in P_{ins}^{inner} , also leads to more branched topology, and an increase in m increases the total number of branches by increasing the number of methyl branches significantly. An increase in P_{ins}^{end} , on the

other hand, indicates that insertion at the chain end is more probable, which leads to formation of longer monomer runs at the chain end and a decrease in the total number of branches.

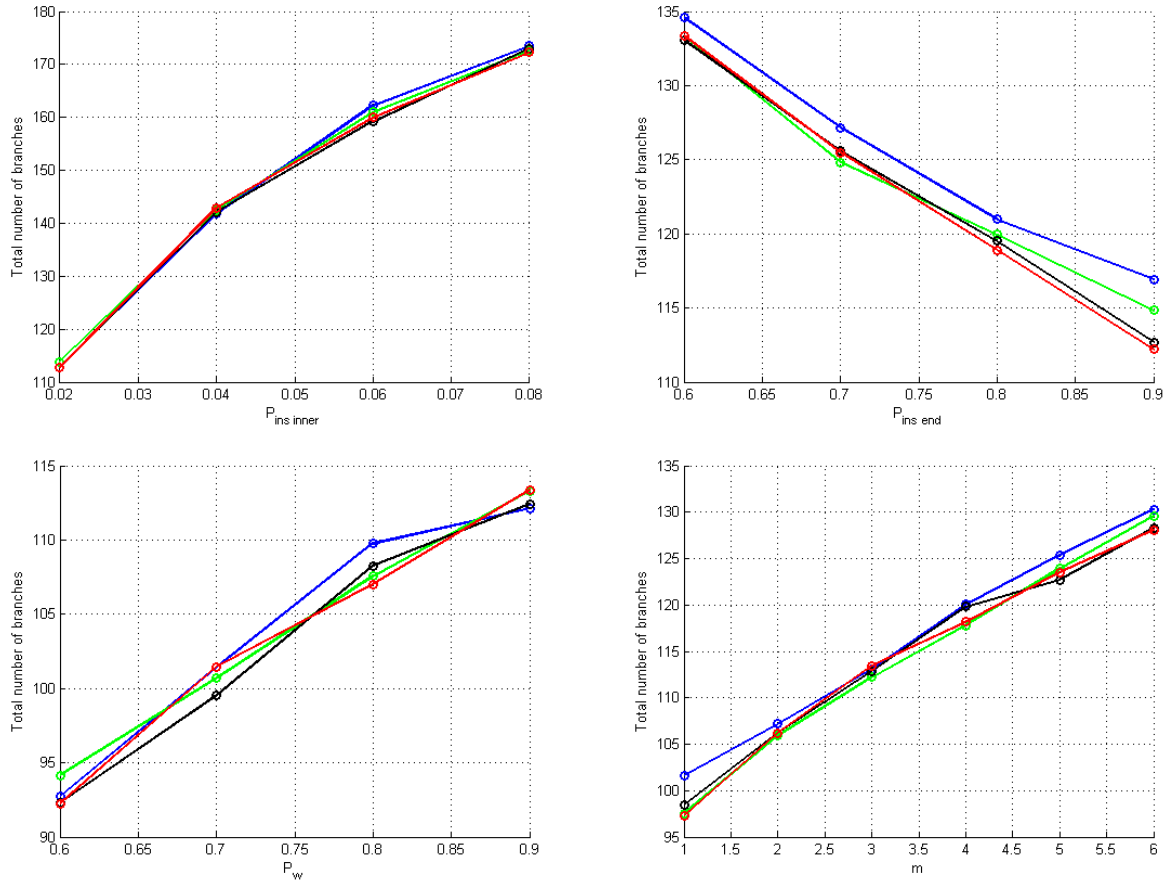


Figure 4-5. Effect of increase in values of P_{ins}^{inner} , P_{ins}^{end} , P_w , and m on average total number of branches per 1000 C of chains for reaction times of 1000s (—), 3000s (—), 5000s (—), and 7000s (—).

The density of total branches reaches equilibrium very early in polymerization, as seen by the low sensitivity of the Figure 4-5 results to reaction time. As shown in Figure 4-6, the average number of branches per 1000 carbon remains constant after about 50s of polymerization, independent of branch length.

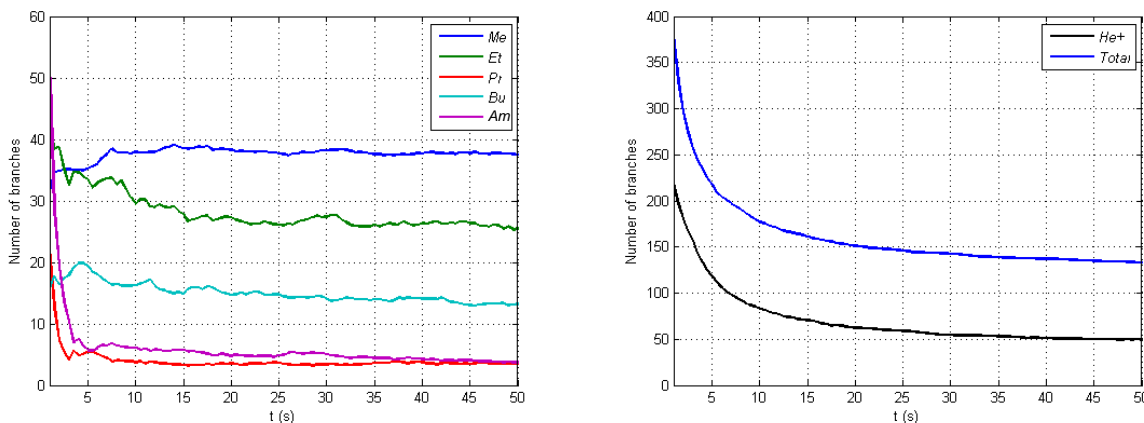


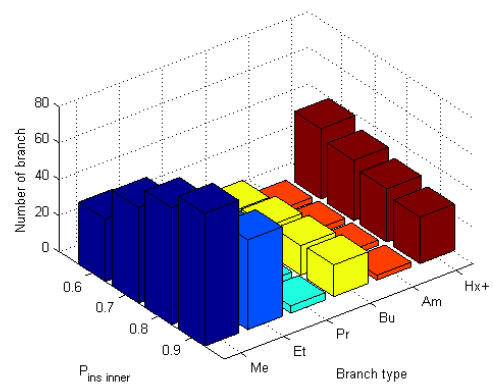
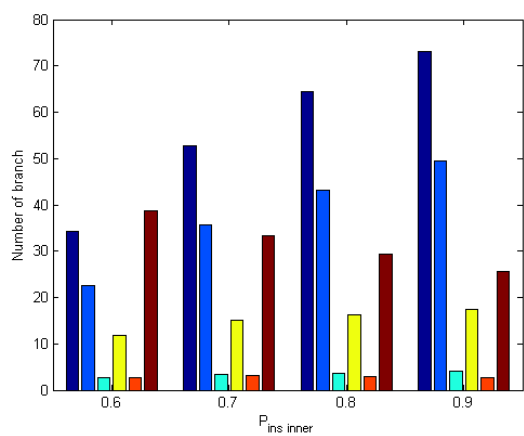
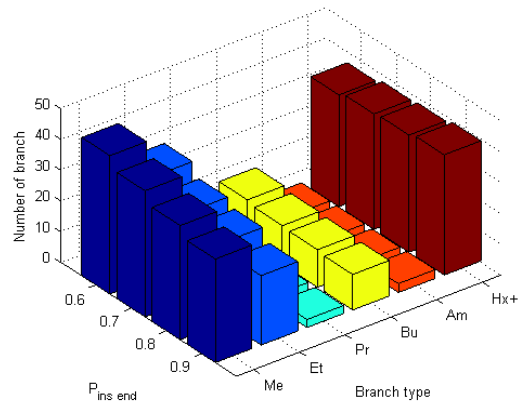
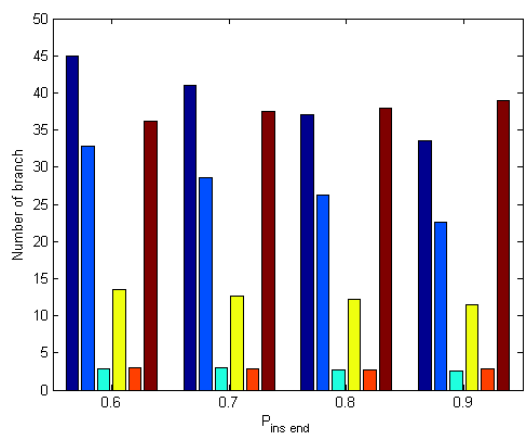
Figure 4-6. Branch density profiles in early stages polymerization. Left figure shows profiles for shorter branches and right figure presents profiles for Hx+ and total number of branches.

4.3.3 Sensitivity Analysis: Branch Distribution

The sensitivity of the distribution of branch lengths to various parameters is summarized by the bar graphs shown as Figure 4-7. Not surprisingly, an increase in P_{ins}^{end} (more monomer insertion at the chain ends) decreases all branch populations, except for the longer branches (Hx+). On the other hand, higher P_{ins}^{inner} increases the density of shorter branches in the chain and decreases the population of Hx+.

The effect of P_w on branch distributions is more complex. The density of methyl groups is not affected considerably by P_w ; the small fluctuations seen are the natural result of randomness behavior of MC method. Ethyl and butyl group populations, however, increase at higher P_w . This observation is in agreement with results generated with Escobedo's algorithm by Chen et al.: "It is observed that for increasing P_w , the population of branches with even number of carbon atoms increases, while that of branches with odd number of carbon atoms decreases."²⁴

Finally, it is seen that the number of methyl branches increases significantly for larger m values. Formation of more methyl groups also provides a situation for ethyl branches to be created. Therefore, higher m will lead to formation of more methyl and ethyl branches.



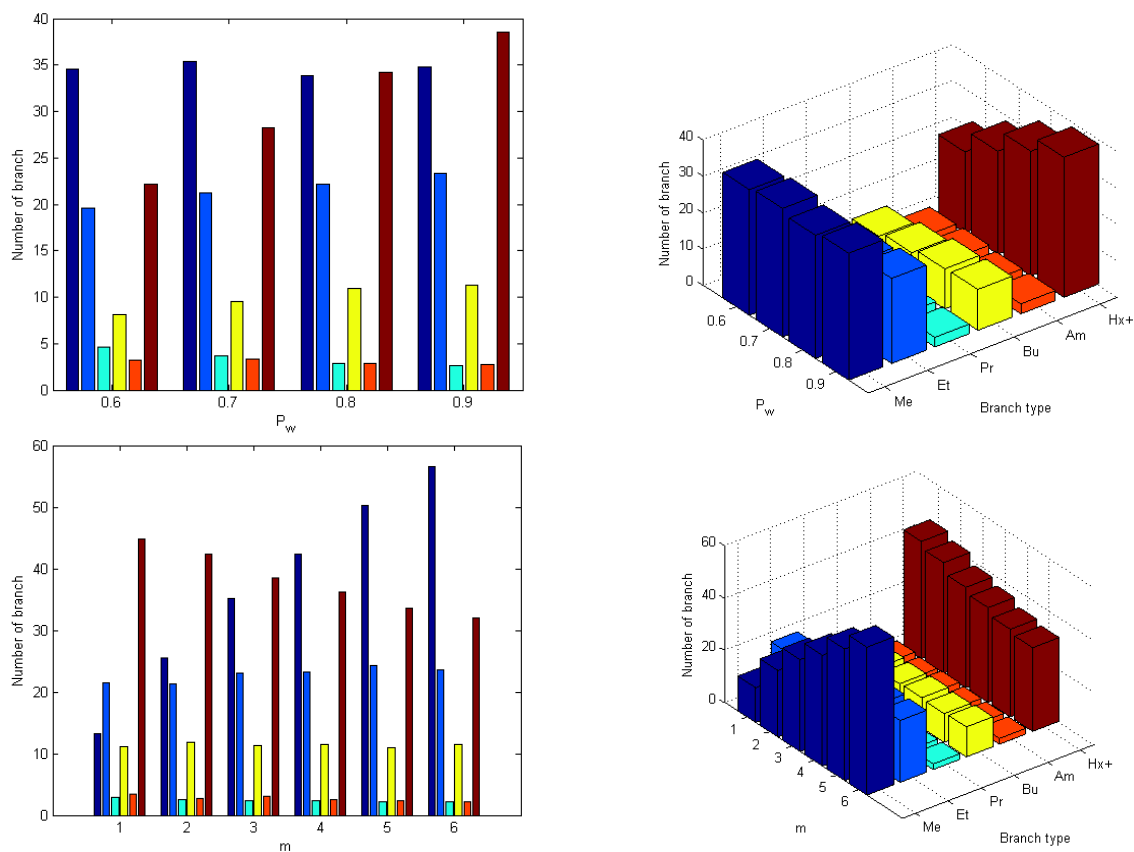


Figure 4-7. Effect of increase in values of P_{ins}^{end} , P_{ins}^{inner} , P_w , and m on branch distribution per 1000 C of chains. Branch type: Me (■), Et (■), Pr (■), Bu (■), Am (■), and Hx+ (■).

The results of the entire sensitivity analysis are summarized in Table 4-4, which was used to guide the adjustment of input parameters to match experimental results. For example, if simulated density of longer branches (Hx+) is greater than found

experimentally, P_w or P_{ins}^{end} will be decreased or P_{ins}^{inner} will be increased, depending on the required density of the shorter branches.

Table 4-4. The effect of input variables on average chain length, total number of branches and branch distribution for ethylene Pd-diimine-catalyzed polymerization, as determined by a sensitivity analysis. Symbols indicate: increase (+), decrease(-), and no change (o). Double symbols show high sensitivity.

Parameter	Effect of increase in the parameters on:							
	Average chain length	Tot. no. of branches	Branch distribution					
			Me	Et	Pr	Bu	Am	Hx+
K_{eq}	-	o	o	o	o	o	o	o
k_{ins}^{end}	++	o	o	o	o	o	o	o
P_{ins}^{end}	--	--	--	--	-	-	-	+
P_{ins}^{inner}	++	++	++	++	+	+	o	--
P_w	--	++	o	+	--	+	-	++
m	-	++	++	+	-	o	-	--

4.3.4 Comparison to Experimental Data

The model described above was run according to the experimental recipes specified in Table 4-5. The combined Escobedo/Gillespie algorithm developed in this study was used in order to consider the experimental polymerization time as well as the polymer structure. Table 4-6 shows the base set of parameters used in the simulations.

Table 4-5. Polymerization conditions of ethylene polymer experiments set by Ye et al. with Pd-catalysts.¹⁶

Polymer	Catalyst amount (μmol)	Ethylene pressure (atm)	Temperature ($^{\circ}\text{C}$)	Time (h)	Solvent (mL CH_2Cl_2)
1	100	1	35	18	100
2	100	1	25	18	100
3	100	6.5	25	19	300
4	90	30	25	5	300

Table 4-6. Set of parameters for simulation of polymerization in Table 4-5.

Input variables						Calculated parameters		
P_w	P_{ins}^{end}	P_{ins}^{inner}	k_{ins}^{end} (s^{-1})	K_{eq} (mol/L)	m	k_w (s^{-1})	k_T^{exp} (L/mol.s)	k_{ins}^{inner} (s^{-1})
0.9	0.9	0.02	50	5×10^{-4}	3	2.3×10^4	1.1×10^4	0.1134

The model shows excellent representation of the distribution of branch-lengths as well as the total number of branches found experimentally for all conditions in Table 4-5, as shown in Table 4-7 and Figure 4-8. The simulated results are average values of branching levels per 1000 C atoms for 100 sample chains in the system. An increase in ethylene pressure from 1 to 30 atm (polymer 2 to polymer 4) leads to a decrease in the simulated total number of branches, in agreement with the experimental results. Without further knowledge about the system, rate coefficients in the simulation were assumed to be independent of temperature. This assumption seems justified within the narrow temperature range examined experimentally, as a

10 °C decrease in temperature (polymer 1 to polymer 2) has only a negligible effect on both the simulated and experimental branch distributions. In the simulation, temperature has a slight effect on results due to its influence on monomer concentration in the solvent.

Table 4-7. Polymer short chain branching distribution and total number of branches per 1000 C from experimental data (measured by ^{13}C NMR in CDCl_3 at 30 °C)¹⁶ and simulation results.

Polymer		Me	Et	Pr	Bu	Am	Hx+	Total
1	<i>Exp</i>	33.7	24.2	2.4	11.5	2.9	37.2	112
	<i>Sim</i>	33.9	22.9	2.6	11.4	2.7	39.5	112
2	<i>Exp</i>	32.9	23.8	2.2	11.4	2.7	37.7	111
	<i>Sim</i>	33.4	23.1	2.6	11.4	2.7	38.2	111
3	<i>Exp</i>	33.0	23.1	3.1	11.3	3.1	35.5	109
	<i>Sim</i>	34.1	22.4	2.9	10.8	3.0	35	108
4	<i>Exp</i>	32.0	19.3	3.5	9.4	3.5	34.2	102
	<i>Sim</i>	33.7	20.0	3.2	10.7	2.9	33.5	104

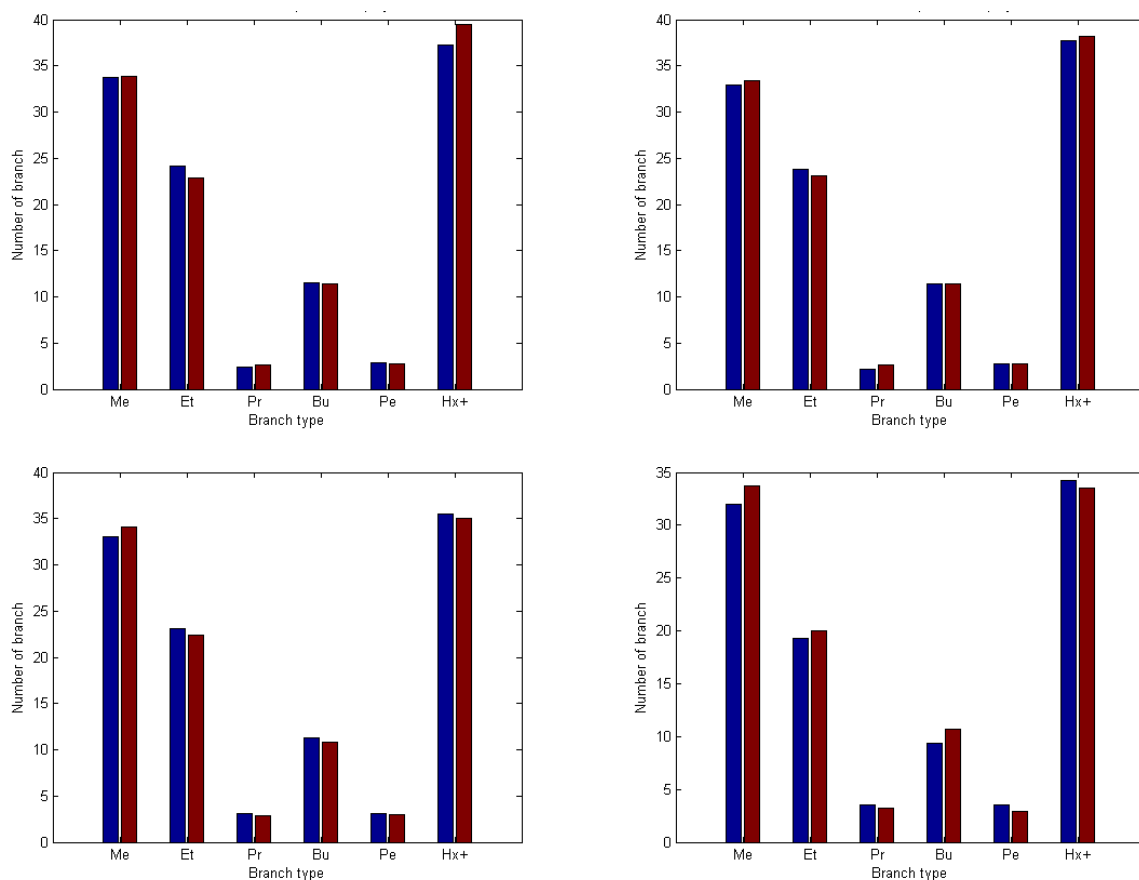


Figure 4-8. Comparison of branch distributions from experimental data (■) and simulation results (■) for each polymer in Table 4-7.

However, the simulation was unable to match the experimental chain lengths attained in the reported polymerization times using the single set of parameters in Table 4-6. It was necessary to adjust k_{ins}^{end} , a coefficient that effects average chain length (Section 4.3.1) but not branching density (Section 4.3.2) of the polymer. The final values used in order to match the simulated degree of polymerization to that for experiments are summarized in Table 4-8. The value of k_{ins}^{end} was more than

doubled in order to match the rate of chain growth at 30 atm (polymer 4) compared to 1 atm (polymer 2), even with the value of $[M]$ also being higher at the higher pressure (0.5647 compared to 0.0189 mol/L at 1 atm). The required change in k_{ins}^{end} with pressure, however, was not systematic, as the value was lowered in order to match the experimental results at 6.5 atm (polymer 3). Further investigation is necessary to determine if this parameter adjustment required indicates a deficiency in the set of mechanisms developed to describe the system, or is just a reflection of typical experimental variation. Note that this mismatch would not be captured by application of the Escobedo's algorithm, which only calculates final polymer structure.

Table 4-8. Comparison of experimental¹⁶ and simulated chain length according to the value of k_{ins}^{end} .

Polymer	No. of Catalyst molecules	Ethylene pressure (atm)	Temp. (°C)	Time (h)	DP_n^{sim}	DP_n^{exp}	k_{ins}^{end} (s^{-1})
1	100	1	35	18	2759	2738	7.0
2	100	1	25	18	2414	2418	6.0
3	100	6.5	25	19	2175	2182	4.3
4	100	30	25	5	2079	2083	14.8

In order to provide a sample visualization of hyperbranched polymers at different conditions, structural information generated by the model (see appendix for more details) was translated to “Simplified Molecular-Input Line-Entry System (SMILES)”

notation, a standard input for molecular mechanics modeling software.^{34,35} In this study, Avogadro's open-source molecular editor was chosen to visualize the chain conformations. Visualization was finalized after implementation of built-in auto optimization tool in Avogadro's software. The toolbox optimised the bond energies by considering the force fields of atoms in the chain and rendered the chain conformations. In the 3D conformations shown in Figure 4-9, branches with the same index number (e.g., same branch level) are distinguished by different colors. It is observed in Figure 4-9 that polymers formed at lower reactor pressure are more branched and have more compact topology.

The visualization and MC conformational studies done by Chen et al.²⁴ are different from the visualization method described above. In that work, the topology was built based on solid volume of hard spheres with a specified diameter. During conformation optimization, a randomly selected bead is displaced in a random direction and if no overlapping occurs and all influenced bonds satisfy the bond-length constraints, the new position of the bead was accepted. Despite this difference in approach, the results of the visualization were the same, with decreased pressure leading to a more highly branched and compact structure.

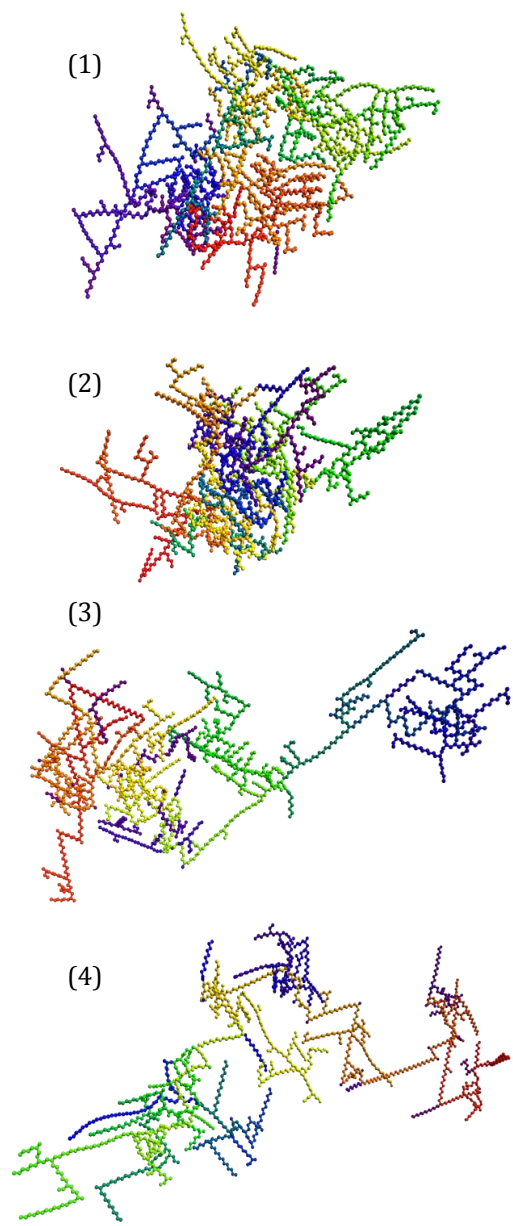


Figure 4-9. Sample snapshots of the conformations of polymer macromolecule in Table 4-5. Each polymer consists of 1500 carbons. Each color represents a

branch index (branching level). Plots (1) to (4) are related to polymer 1 to 4 in Table 4-5, respectively.

4.3.5 Effect of Changing Pressure During Polymerization

In order to investigate the effect of changing pressure during polymerization to tune the chain topology, two different scenarios were studied. In the first scenario, polymerization is started with low pressure to form a hyperbranched topology, and then at a specific time, pressure is increased suddenly to create a more linear chain section. In the second scenario, the linear section is formed at the high pressure first, followed by a sudden drop in pressure to allow hyperbranched material to be formed. Figure 4-10 shows the topology visualization of a sample chain for the two scenarios before the pressure change and at the end of polymerization.

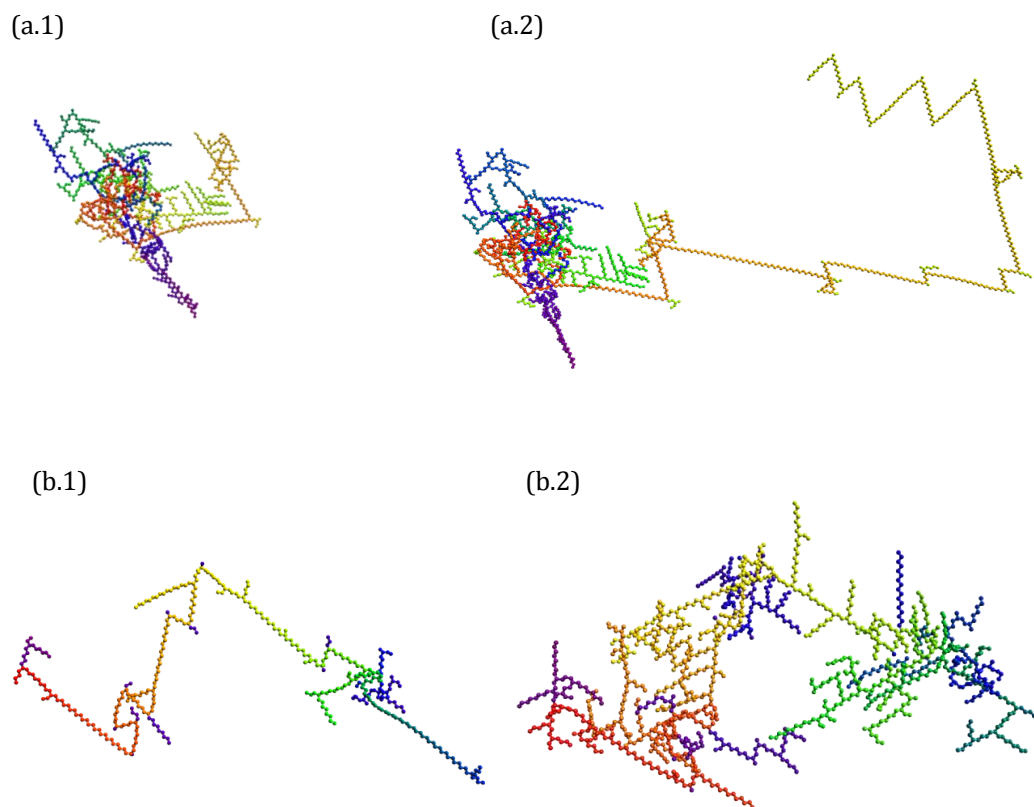


Figure 4-10. Sample snapshots of the chain produced in two scenarios: (a) chain formed initially at 1 atm (a.1) followed by further chain growth at 100 atm (a.2); and (b) chain formed initially at 100 atm (b.1) followed by further chain growth at 1 atm (b.2).

As seen in Figure 4-10a, the chain formed by the first scenario consists of two different topological sections in which one end is more hyperbranched and the other is more linear. The sudden increase in the pressure after the formation of the hyperbranched structure leads to formation of a more linear section in which

branch-on-branch structure is reduced due to the higher concentration of monomer and consequently, higher probability of dissociation that favors insertion over chain walking. On the other hand, for the second case, a linear section is formed initially at high pressure. Upon reduction of the pressure, the chain spends more time in the active state, favoring chain walking over insertion; as seen in Figure 4-10b, the increased branching that occurs is distributed over the entire chain (including the original more linear portion), as the catalyst center can move back and create branches on the part of the chain formed at high pressure. These qualitative results from simulation are comparable with experimental observation.³³ Xiang et al. discovered an alternative way to tune the topology of the hyperbranched polymers and eliminate the phenomenon simulated in scenario 2 by adding aliphatic rings to the system (provided by a comonomer) to block metal site migration; simulation of this innovation will be left for future studies.

4.4 Conclusion

Four major events in polymerization of ethylene with Pd-diimine catalyst were introduced. A hybrid model was developed combining Escobedo's and Gillespie's algorithms. The new model had the ability to track chain growth as a function of the polymerization time by considering the absolute values of coefficients and reaction rates. A sensitivity analysis of input variables (K_{eq} , k_{ins}^{end} , P_{ins}^{end} , P_{ins}^{inner} , P_w , and m)

demonstrated that an increase in k_{ins}^{end} or P_{ins}^{inner} causes longer average chain length while an increase in other input parameters leads to shorter average chain length. It was also seen that the total number of branches increases for higher values of P_{ins}^{inner} , P_w , and m and for lower values of P_{ins}^{end} . The model was utilized to simulate the branch density profile for early stages of polymerization.

The input parameters were set at values that provided a good description of the experimental studies of Ye et al. The simulated results were compared to experimental results at four different conditions and excellent agreement between results in branch distribution was achieved. In addition and in contrast to Escobedo's algorithm, the overall evolution of chain length with time was captured, which allows the consideration of reaction scenarios such as the change in pressure. Sample snapshots of final chain topologies for each of the comparing conditions were rendered by employing the molecular editor software package, Avogadro.

References

- (1) Webster, O. W. *Science* **1991**, *251*, 887–893.
- (2) Bosman, A. W.; Janssen, H. M.; Meijer, E. W. *Chem. Rev.* **1999**, *99*, 1665–1688.
- (3) Fischer, M.; Vögtle, F. *Angew. Chemie Int. Ed.* **1999**, *38*, 884–905.
- (4) Fréchet, J. M. *Science* **1994**, *263*, 1710–1715.
- (5) Fréchet, J. M.; Henmi, M.; Gitsov, I.; Aoshima, S.; Leduc, M. R.; Grubbs, R. B. *Science* **1995**, *269*, 1080–1083.
- (6) Kämpfen, Y. *Biomed. Tech. (Berl)*. **1975**, *20*, 150–154.
- (7) G. Odian. *Principles of Polymerization*; WILEY: New York, 1991.
- (8) Kim, Y. H. *J. Polym. Sci. Part A Polym. Chem.* **1998**, *36*, 1685–1698.
- (9) Dong, Z.; Ye, Z. *Polym. Chem.* **2012**, *3*, 286.
- (10) Guan, Z. .; Cotts, P. M. .; McCord, E. F. .; McLain, S. J. *Science*. **1999**, *283*, 2059–2062.
- (11) Ittel, S. D.; Johnson, L. K.; Brookhart, M. *Chem. Rev.* **2000**, *100*, 1169–1204.
- (12) Guan, Z. .; Cotts, P. M. .; McCord, E. F. .; McLain, S. J. *Science*. **1999**, *283*, 2059–2062.
- (13) Ye, Z.; Li, S. *Macromol. React. Eng.* **2010**, *4*, 319–332.
- (14) Johnson, L. K.; Killian, C. M.; Brookhart, M. *J. Am. Chem. Soc.* **1995**, *117*, 6414–6415.
- (15) Usami, T.; Takayama, S. *Macromolecules* **1984**, *17*, 1756–1761.
- (16) Ye, Z.; Zhu, S. *Macromolecules* **2003**, *36*, 2194–2197.
- (17) Johnson, L. K.; Killian, C. M.; Brookhart, M. *J. Am. Chem. Soc.* **1995**, *117*, 6414–6415.

- (18) Tempel, D. J.; Johnson, L. K.; Huff, R. L.; White, P. S.; Brookhart, M. J. *Am. Chem. Soc.* **2000**, *122*, 6686–6700.
- (19) Cotts, P. M.; Guan, Z.; McCord, E.; McLain, S. *Macromolecules* **2000**, *33*, 6945–6952.
- (20) Mansfield, M. L.; Klushin, L. I. *Macromolecules* **1993**, *26*, 4262–4268.
- (21) Kłos, J. S.; Sommer, J.-U. *Macromolecules* **2013**, *46*, 3107–3117.
- (22) Kłos, J. S.; Sommer, J.-U. *Macromolecules* **2009**, *42*, 4878–4886.
- (23) Wawrzyńska, E.; Eisenhaber, S.; Parzuchowski, P.; Sikorski, A.; Zifferer, G. *Macromol. Theory Simulations* **2014**, *23*, 288–299.
- (24) Chen, Z.; Gospodinov, I.; Escobedo, F. A. *Macromol. Theory Simulations* **2002**, *11*, 136–146.
- (25) Galland, G. B.; de Souza, R. F.; Mauler, R. S.; Nunes, F. F. *Macromolecules* **1999**, *32*, 1620–1625.
- (26) Jurkiewicz, A.; Eilerts, N. W.; Hsieh, E. T. *Macromolecules* **1999**, *32*, 5471–5476.
- (27) Simon, L. .; de Souza, R. .; Soares, J. B. .; Mauler, R. . *Polymer (Guildf)*. **2001**, *42*, 4885–4892.
- (28) McLain, S. J.; McCord, E. F.; Johnson, L. K.; Ittel, S. D.; Nelson, T. J.; Arthur, S. D.; Halfhill, M. J.; Teasley, M. F. *Polym. Prep.* **1997**, *38*, 772.
- (29) Möhring, V. M.; Fink, G. *Angew. Chemie Int. Ed. English* **1985**, *24*, 1001–1003.
- (30) Gillespie, D. T. *J. Comput. Phys.* **1976**, *22*, 403–434.
- (31) Smith, J. M.; Van Ness, H. C.; Abbott, M. M. *Introduction to chemical engineering thermodynamics*; McGraw-Hill: New York, 2005; Vol. 27, pp. 350–356.
- (32) Michels, A.; Wassenaar, T. *Physica* **1950**, *16*, 221–224.
- (33) Xiang, P.; Ye, Z.; Morgan, S.; Xia, X.; Liu, W. *Macromolecules* **2009**, *42*, 4946–4949.

- (34) Weininger, D. *J. Chem. Inf. Model.* **1988**, *28*, 31–36.
- (35) Weininger, D.; Weininger, A.; Weininger, J. L. *J. Chem. Inf. Model.* **1989**, *29*, 97–101.

Chapter 5

Conclusions and Future Work

The Monte Carlo method, a stochastic technique, was shown to be a powerful tool to simulate polymerization kinetics in which randomness is a natural behavior. It provides detailed information of the distributions of chain microstructure and is conceptually straight forward to implement, at the expense of long computing time.

The Gillespie MC method was combined with a deterministic technique in a hybrid algorithm in order to investigate the distribution of functional groups within the polymer molecular weight distribution produced by semibatch free radical polymerization. The deterministic methods examined, either original or extended counters model, were unable to track chains with a higher level of functional groups. The MC method, however, provided the full molecular distribution of chains with any number of functional groups. Implementing the MC technique, it was observed that only a quarter of the chains produced have the desired composition of a single functional group per polymer molecule and that approximately half of the chains synthesized containing no functional groups. The hybrid model, implemented in PREDICI11, has the advantages of both simulation methods. It benefits from the simple basic model formulation and short simulation time of the Galerkin-h-p deterministic technique (applied in the software package PREDICI); and also provides the detailed information of the polymer chain microstructure generated by the MC approach.

Another example of combined MC methods was formulated to simulate the ethylene polymerization with Pd-diimine catalyst, wherein hyperbranched molecules are synthesized through a chain-walking mechanism. One MC approach based on fixed probabilities, Escobedo's algorithm, was implemented in order to study the conformations of isolated molecules to relate molecular shape and topology. However, as Escobedo's algorithm was constructed using relative probabilities, it was unable to simulate chain growth as a function of polymerization time or changing reaction conditions. Thus, Escobedo's algorithm was extended with a well-known MC technique, Gillespie's algorithm to consider absolute rates of reactions.

The effect of input variables on the chain distribution, average chain length, and total number of branches was then examined in a sensitivity study. It was observed that after fewer than 100 seconds, the branch distribution of the chains reaches to equilibrium and does not change with time, and that an increase in ethylene pressure caused less branched polymer chains as expected. The dynamic capabilities of the new algorithm were demonstrated by considering scenarios where ethylene pressure underwent a step change during polymer chain formation.

As a possible extension of the modeling described in Chapter 3, one can add kinetics complexities such as acrylate backbiting and reactions of macromonomers, taking advantage of the capabilities of the software package PREDICI to completely describe high temperature polymerization of multimonomer systems.¹ With the MC capabilities of the hybrid technique, the program can still calculate functional

group incorporation as a function of chain length for complex systems. Thus, the model can be used to simulate the distribution of functionalities during production of reactive dispersants used to stabilize nanoparticles produced by non-aqueous dispersion polymerization, in support of the experimental investigation by PhD candidate Weiwei Yang in Prof. Hutchinson's group.

In ethylene hyperbranched polymerization, the model can be used as a basis to consider situations of interest to Prof. Ye's group, including the possible extension to copolymerization or to investigate the effect of adding a blocking unit to the recipe. In addition, the model can be extended in order to calculate molecular properties such as radius of gyration.

References

- (1) Wang, W.; Hutchinson, R. A. *AIChE J.* **2011**, *57*, 227–238.

Appendix

The algorithms describing the polymerizations discussed in Chapters 3 and 4 of this research are implemented in the programming software, MATLAB® 2013b, and 2014a. Although in comparison to other programming languages/software such as C/C++, FORTRAN, and Visual Basic, simulation time in MATLAB® may be longer, the package provides a robust platform for systems for which fast-indexing and handling matrices are required. In addition, user-friendly command window and no need to call function libraries are advantages of programming in MATLAB®.

The programming of simulation of hyper-branched polymerization, described in Chapter 4, demands a solution for labeling carbons in the chain in order to reconstruct the branching structure. The common method for labeling branched polymerization is to label each monomer. With this method, it is possible to store the number of the starting monomer of a branch, as a branch number, into a matrix. By adding the length of branch to the respective branch number, one can have topology information of a branched chain while consuming only small amount of memory. In other words, each monomer has its own number, but it is not stored; only the monomer number of parent branch at connection point and respective branch length are saved. For example, Figure A-1 shows the schematic topology of a chain with length of 80:

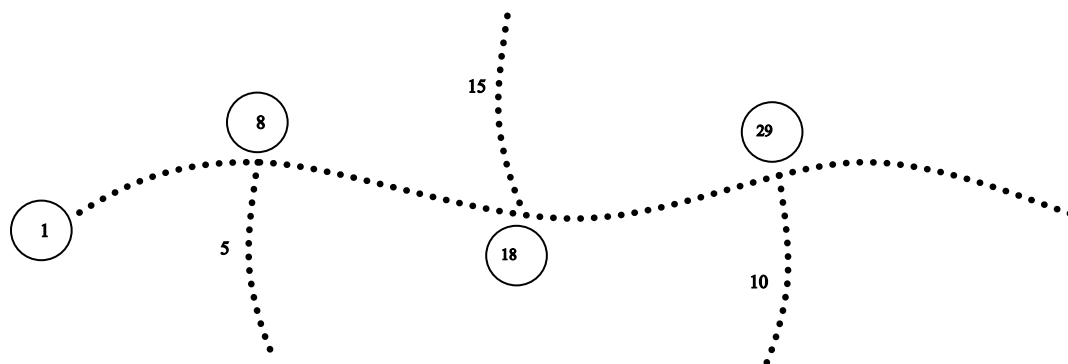


Figure A-1. Sample schematic chain topology of a chain with length of 80. Numbers in the circle show the label of the parent monomer, and numbers without symbols display the branch length.

The structure information of the chain is stored in the matrix (A.1):

$$struc_info = \begin{bmatrix} 1 & 50 \\ 8 & 5 \\ 18 & 15 \\ 29 & 10 \end{bmatrix} \quad (A.1)$$

where the first column is the branch number (the label of parent monomer) and the second column is the length of branch.

It was seen that these two indexes are not enough to track the topology changes in chain walking polymerization since the catalyst center moves along all of the branches (and the backbone). If the catalyst center is on inner segments and insertion happens, the labeling of a new branch number would be an issue because: first, the monomer label where the catalyst center is located, is not stored in

advance and cannot be calculated later; and second, the label of the new monomer is incompatible as a label for new branch.

Hence, a new parameter was introduced to resolve this issue. “Last monomer label of the branch” or “last monomer label” in short, helps to find the label of the monomer where the catalyst center is located. Without this factor, it was not possible to find the branch containing the catalyst center which is required in order to calculate f, m (correction factors in Chapter 4) and the next potential location of the catalyst center if chain walking occurs. Moreover, last monomer label helps to determine the sequence of branch creation, which is an important key in visualization of the chain.

By adding a new parameter, the Figure A-1 and its corresponding matrix convert to Figure A-2 and matrix (A.2):

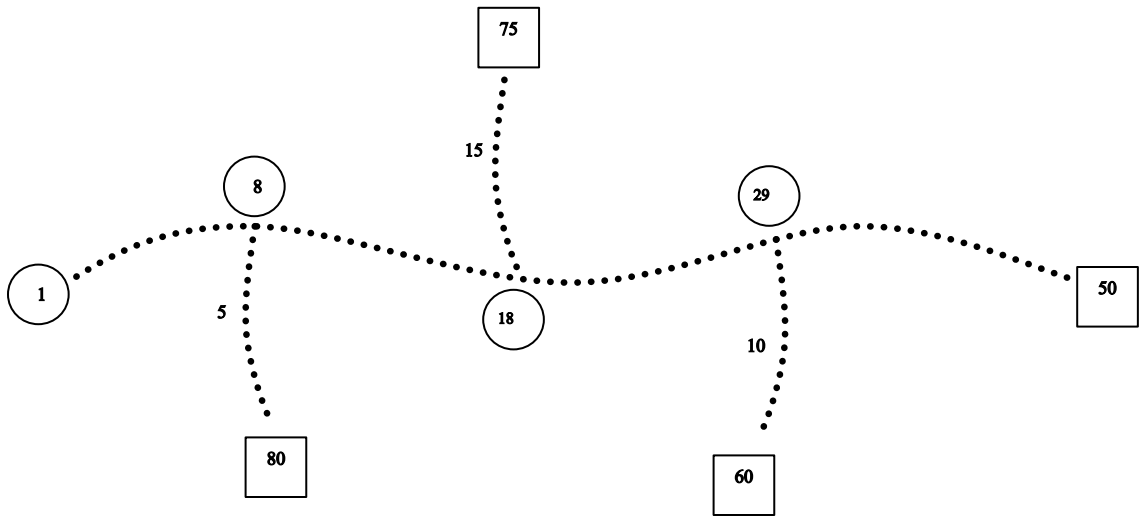


Figure A-2. Sample schematic chain topology of a chain with length of 80.

Numbers in the circle show the label of the parent monomer, numbers in the box show the last monomer label, and numbers without symbols display the branch length.

$$struc_info = \begin{bmatrix} 1 & 50 & 50 \\ 8 & 5 & 80 \\ 18 & 15 & 75 \\ 29 & 10 & 60 \end{bmatrix} \quad (A.2)$$

Therefore, it is possible to find the label of every monomer in the chain and sequence of branch creation. For instance in the example chain, first branch 29 has been created, followed by formation of branch 18 and finally branch 8.